Title
Transcription factors Tbx21 and Bhlhe40 are critical for CD4+ T cell function

Author
Esensten, Jonathan Haynes

Publication Date
2010

Peer reviewed|Thesis/dissertation

Transcription factors Tbx21 and Bhlhe40 are critical for CD4+ T cell function

by

Jonathan Haynes Esensten

DISSERTATION

Submitted in partial satisfaction of the requirements for the degree of

DOCTOR OF PHILOSOPHY
in

Biomedical Sciences / Immunology

in the

GRADUATE DIVISION

of the

UNIVERSITY OF CALIFORNIA, SAN FRANCISCO

Acknowledgements

I thank the many members of the Bluestone lab over the past 5 years who contributed to this work by teaching me techniques and suggesting experiments in many helpful discussions. I thank the Medical Scientist Training Program and the Biomedical Sciences Program for funding and support. It is a privilege and honor to be a part of these programs. The members of my dissertation committee, led by chairman Abul Abbas, have been valued advisors and role models for me. I thank them for their invaluable help and support.

Of course, I thank Jeff Bluestone for his mentorship and support. It has been my honor and privilege to work in his lab. I have learned much immunology from him. More importantly, I have developed a profound respect for the creative vision and relentless drive necessary to turn discoveries about basic biology into treatments for human disease.

The text of this dissertation includes material as it appears in Esensten et al. "T-bet-Deficient NOD Mice Are Protected from Diabetes Due to Defects in Both T Cell and Innate Immune System Function." *Journal of Immunology*, 2009, 183: 75-82. (doi:10.4049/jimmunol.0804154) This material is reprinted with the written permission of the American Association of Immunologists. Copyright 2009. The American Association of Immunologists, Inc. Jeffrey A. Bluestone directed and supervised the work described in this dissertation.

Statement from the research advisor

Chapter 2 is taken from the manuscript Esensten et al," A transcriptional fingerprint of CD28 costimulation in naive human CD4+ T cells reveals a role for BHLHBE40 transcription factor in costimulation," Jonathan H. Esensten planned and carried out all experiments, with the following exceptions: The work describing thymic and peripheral T cell phenotypes in Bhlhe40 -/- mice, mentioned in the discussion section, which were carried out by co-author Dennis D. Taub[1]. Co-authors Marc Martinez Llordella[2] and Ann Marini[3] provided assistance with mouse T cell activation experiments described in Figure 5 and supplemental Figure 3. Co-author Robert H. Lipsky[4] made the *Bhlhe40 -/-* mice and arranged for them to be shipped to us.

Chapter 3 is taken from the publication Esensten et al. "T-bet-Deficient NOD Mice Are Protected from Diabetes Due to Defects in Both T Cell and Innate Immune System Function." *Journal of Immunology*, 2009, 183: 75-82, Jonathan H. Esensten planned and carried out all experiments except for the diabetes incidence experiments in Figure 1, which were carried out by co-author Michael R. Lee. Co-author Laurie A. Glimcher provided the Tbx21-null mouse used in this work. The manuscript was written by J.H.E. All author affiliations are available in the published paper.

I directed and supervised all the above work. These publications and manuscript form a body of knowledge that makes original contributions to scientific knowledge. As such, this

---

[1] Laboratory of Immunology, National Institute on Aging-Intramural Research Program, National Institutes of Health, Baltimore, MD 21224, USA.
[2] Diabetes Center and the Department of Medicine, University of California, San Francisco, San Francisco, California 94143, USA
[3] Department of Neurology and Neuroscience Program, Uniformed Services University of the Health Sciences, Bethesda, Maryland 20814, USA.
[4] Department of Neurosciences, Inova Health System, Inova Fairfax Hospital. 3300 Gallows Road. Falls Church, VA 22042

dissertation meets the standard for a doctoral dissertation in the Biomedical Sciences Program at the University of California, San Francisco.

Jeffrey A. Bluestone, PhD

Title: Transcription factors Tbx21 and Bhlhe40 are critical for CD4+ T cell function

By Jonathan Haynes Esensten

Abstract

CD4+ T cells can take on a wide variety of effector phenotypes. Over the past 10 years, many different transcription factors have been identified that direct CD4+ T cell subphenotypes by initiating and sustaining unique transcriptional programs. Below, I show that expression of the transcription factor Tbx21 (T-bet) is necessary for diabetes in the NOD mouse. Expression of the transcription factor in both T cells and antigen presenting cells is necessary for disease in adoptive transfer models of autoimmune diabetes. Further, I show that *Tbx21-/-* regulatory T cells are competent to prevent diabetes in *NOD.Cd28 -/-* mice, which have greatly reduced Treg levels. Like Tbx21, CD28 is also critical for T cell activation and effector T cell differentiation. In an attempt to further understand the effect of CD28 ligation on effector cell activation, I activated naive human CD4+ T cells and measured global transcriptional changes by using microarray analysis. I found that at 4 hours after activation, CD28 ligation mostly amplified the changes initiated by TCR ligation. However, by 24 hours after activation, CD28 ligation was necessary to prevent global transcriptional quiescence. From these microarray data, I identified the transcription factor Bhlhe40 as a highly CD28-dependent gene. I show that the transcription factor is necessary for CD28 costimulation-dependent phenotypes such as CD25 expression in Jurkat T cells and IL-2 expression in primary mouse CD4+ T cells. Thus, I have identified a novel role for Bhlhe40 in CD28 costimulation during T cell activation and demonstrated a mechanism for the qualitative effects of CD28 costimulation.

Table of Contents

List of Figures

List of Tables

Chapter 1: General Introduction

Effective adaptive immune responses against pathogens require productive activation of CD4+ T cells in secondary lymphoid tissues. After activation, clonal expansion and differentiation into a phenotypically distinct T cell subset allows for the effective elimination of a wide variety of different pathogens. In patients with autoimmune disease, the adaptive immune response targets autoantigens, leading to tissue destruction or chronic inflammation. How are the cell fate decisions made that drive a CD4+ T cell toward a particular effector phenotype? Below, I discuss the central findings and implications of two major projects that I have done that explore this question from the perspective of specific transcription factors. Transcriptional regulation is central to CD4+ cell fate decisions in the thymus (1) and in post-thymic development of effector T cell subsets such as Th1, Th2, Th17, and Tregs (2,3). Over the past 10 years, specific transcription factors have been linked to a wide variety of CD4+ T cell differentiation decisions. For example, the transcription factor Th-POK directs CD4+ T cell fate in the thymus(4) and the transcription factor Foxp3 further specifies the phenotype of regulatory T cells (5).

In the work described below, I have focused on two transcription factors involved in different aspects of T cell activation and effector cell function: 1) the transcription factor Bhlhe40, which I show is necessary for normal transcriptional responses to CD28 costimulation, and 2) the transcription factor Tbx21 (T-bet), which I show is necessary for normal CD4+ T cell function and normal antigen presenting cell function in adoptive transfer models of autoimmune diabetes. Tbx21 is also required for spontaneous autoimmune diabetes in the NOD mouse. This work contributes to a fuller understanding of the diversity of CD4+ T cell phenotypes and the requirements for CD4+ T cell function during normal activation and autoimmunity. Each of the two chapters (2 and 3) presenting original experimental data includes independent introductions to the specific background and context of the work described. In the general discussion in chapter

4, I review the impact of the research described in this dissertation and explore some of the avenues for future research on the roles of transcription factors in directing T cell activation and effector phenotypes.

References

1. Rothenberg, E. V., J. E. Moore, and M. A. Yui. 2008. Launching the T-cell-lineage developmental programme. *Nat. Rev. Immunol.* 8: 9-21.

2. Zhu, J. and W. E. Paul. 2008. CD4 T cells: fates, functions, and faults. *Blood* 112: 1557-1569.

3. Wan, Y. Y. and R. A. Flavell. 2009. How diverse--CD4 effector T cells and their functions. *J. Mol. Cell. Biol.* 1: 20-36.

4. He, X., X. He, V. P. Dave, Y. Zhang, X. Hua, E. Nicolas, W. Xu, B. A. Roe, and D. J. Kappes. 2005. The zinc finger transcription factor Th-POK regulates CD4 versus CD8 T-cell lineage commitment. *Nature* 433: 826-833.

5. Fontenot, J. D., M. A. Gavin, and A. Y. Rudensky. 2003. Foxp3 programs the development and function of CD4+CD25+ regulatory T cells. *Nat. Immunol.* 4: 330-336.

Chapter 2: A transcriptional fingerprint of CD28 costimulation in naive human CD4+ T cells reveals a role for BHLHBE40 transcription factor in costimulation

This chapter is a manuscript in preparation. Please see the statement from the research advisor for the contributions and institutional affiliations of the co-authors.

Abstract

Productive CD4+ T cell activation requires both an antigen-specific signal through the T cell receptor and a costimulatory signal via the CD28 receptor. Although the membrane-proximal signaling events downstream of CD28 ligation have been extensively studied, little is known about how those signals direct the extensive changes in global gene transcription after T cell activation. In this paper, we define the global transcriptional effects of CD28 costimulation with microarray expression analysis. We demonstrate that CD28 costimulation has quantitative effects on genome-wide transcription in the first several hours after activation, but strong qualitative effects on transcription by 24 hours after activation. Further, we identify a transcription factor, Bhlhe40, that is highly induced by CD28 costimulation and is necessary for maximal transcription of IL-2 and Bclxl, two highly CD28-dependent genes. Finally, we show that Bhlhe40 is necessary for maximal disease in MOG peptide-induced experimental autoimmune encephalitis in the mouse, validating the *in vivo* importance of this gene for immune system function in a CD28-dependent disease.

Introduction

For productive activation, T cells require two signals: an antigen-specific signal through the T cell receptor and a second signal via a costimulatory receptor. CD28 is a critical costimulatory receptor for naive CD4+ T cells (1). TCR ligation in concert with engagement of CD28 by its ligands CD80 and CD86 leads to sustained proliferation and production of IL-2, protection from apoptosis, and differentiation toward T-effector phenotypes (reviewed in (1)). TCR ligation in the absence of CD28 induces anergy in T cells (2, 3). Although costimulation via CD28 has been widely studied in both *in vivo* and *in vitro* models, it is still unclear precisely how the CD28 ligation at the cell surface can induce dramatic phenotypic changes in a T cell (4, 5).

Many different mechanisms have been proposed to explain how CD28 ligation affects T cell activation. These mechanisms fall broadly into the categories of 1) augmenting positive TCR signals (6,7,8,9,10) changing the balance of positive activation signals to promote productive activation and prevent anergy (11,12) blocking proteins such as E3 ubiquitin ligases such as Cbl-b (13) that promote anergy. However, many of these mechanistic studies on CD28 costimulation use cell lines, which have similar but not identical signaling machinery to primary T cells (14). The use of primary cells is complicated by heterogeneity among memory versus naive cells, which have different requirements for costimulation (15, 16).

Instead of focusing on membrane-proximal signaling events and specific transcription factors, some groups have done microarray studies to attempt to understand the difference that CD28 costimulation makes to global transcription. Two published microarray studies probed the role of costimulation in global mRNA transcription after human T cell activation (17, 18). Both of these studies come to similar conclusions: costimulation via CD28 causes distinct differences in expression of a small subset of genes, but generally amplifies the program of global transcription initiated by TCR ligation alone. These conclusions are limited in scope for a few

reasons. First, the populations of cells used in these studies were Jurkat cells, whole primary human peripheral blood T cells, or primary human peripheral blood CD4+ T cells. These cell lines and primary cell populations are not ideal for studies on costimulation via CD28 as described above (19). Second, if the T cells were sub-optimally stimulated, clear qualitative differences induced by CD28 ligation would be difficult to detect. Finally, donor-to-donor variation affects T cell activation, and there is clear evidence of strong person-to-person variation in gene expression in peripheral blood leukocytes (20, 21). Thus, we took these factors into account to build on the existing literature on costimulation-induced transcriptional profiles in primary naive human CD4+ T cells. Such data may help elucidate the CD28-sensitive genes that induce and maintain the phenotype of a costimulated T cell.

In contrast to previous microarray studies of CD28 costimulation, we present data showing that a lack of costimulation induces profound genome-wide transcriptional quiescence by 24 hours after activation, but not at 4 hours after activation of primary naive human CD4+ T cells. CD28 costimulation strongly augments the expression of a few genes (such as IL-2) in the first few hours after activation but has a modest effect on most transcripts. However, by 24 hours, costimulation has a strong qualitative effect on transcription thousands of genes. We also show that the transcriptional profile of a T cell that has received costimulation is not dependent upon the autocrine production of IL-2 in the first 24 hours after activation. Of the genes that were the most costimulation-dependent, we focused on the transcription factor BHLHE40, which we show is critical for maximal IL-2 production after costimulation in Jurkat T cells. Primary mouse CD4+ T cells that lack Bhlhe40 have 30-50% lower levels of Il-2 and Bclxl transcript after activation. *Bhlhe40 +/-* mice are partially protected from experimental autoimmune encephalitis, a highly CD28 costimulation-dependent disease. Thus, we report a novel mechanism for transcription of CD28-dependent genes after T cell activation.

Results

Naive human T cells can be activated with TCR signals alone.

To probe the CD28 costimulation requirements for activation of naive human CD4+ T cells, CD4+CD45RA+ cells were sorted to >99% purity and activated with beads conjugated to anti-CD3 (TCR signal) or anti-CD3 and anti-CD28 (TCR signal with costimulation). Antibody concentrations were titrated to induce maximal cell surface expression of CD69 by 24 hours after activation. The activation profile of T cells from a representative donor is shown in Figure 2.1A. Cells from some donors activated with anti-CD3 alone showed considerable heterogeneity in CD69 staining. Since our aim is to compare populations maximally activated with or without CD28 costimulation, we chose for further analysis three donors that had >50% CD69+ cells in the group treated with anti-CD3 alone (Figure 2.1B). This selection ensures that differences in expression seen in microarray analysis are due to CD28 costimulatory signals and not due to sample heterogeneity. Cell surface activation marker expression data for all 6 donors is in Supplemental Figure 2.1.

CD28 costimulation maintains the transcriptional profile of activation

Expression microarray analysis was performed on RNA samples from the three donors whose activation profiles are shown in Figure 2.1B. Average expression values for each transcript were used for subsequent analysis. The microarray data were confirmed via real-time PCR analysis of a panel of CD28-costimulation dependent genes with the same RNA samples (Supplemental Figure 2.2). The overall mRNA expression profiles of the cells activated for 4 hours shows that a small subset of genes is highly upregulated at this early time point and that this upregulation is not dependent on CD28 costimulation. For example, the transcripts for TNF, EGR1, GEM, NR4A3, and FOSL2 were highly upregulated at 4 hours in cells activated both with and without CD28 (Figure 2.1C, left panels). By contrast, IL-2 expression was highly CD28-

dependent even at 4 hours after activation. IL-2 was a member of only 32 unique transcripts that were >5-fold upregulated by costimulation at both 4 and 24 hours after activation (Table 2.1). By 24 hours after activation, cells that had not received costimulation showed a relatively small number of transcripts that were more than 5-fold differentially expressed compared to cells that had never been activated. By contrast, CD28-costimulated cells showed hundreds of genes with large differences in expression compared to the control unactivated cells (Figure 2.1C, right panels). In particular, cells analyzed at 4 hours after activation showed 350 transcripts were upregulated >5-fold with anti-CD3 stimulation alone (348 with false discovery rate [FDR] adjusted $p<0.05$), compared to control. A total of 807 (804 with FDR-adjusted $p<0.05$) transcripts were upregulated >5-fold with anti-CD3 and CD28 stimulation. By 24 hours after activation, cells that were activated with anti-CD3 and anti-CD28 showed 1127 transcripts with >5-fold upregulation (1113 with FDR-adjusted $p<0.05$), compared to 93 transcripts with >5-fold upregulation (92 with FDR-adjusted $p<0.05$) in cells that were activated with anti-CD3 alone (Figure 2.1C). Thus, CD28 costimulation is more critical at 24 hours than at 4 hours after activation to induce and maintain high levels of transcription. The data in the arrays were validated on the same RNA samples via quantitative real-time PCR using 7 Taqman primer-probes to detect transcripts that were highly up- or down-regulated in the array data (Supplemental Figure 2.2).

CD28-dependent genes are involved in cellular metabolism

To more directly visualize the effects of CD28 costimulation on T cell activation, the transcriptional profile of cells activated with anti-CD3 alone was compared to cells activated with anti-CD3 and anti-CD28 (Figure 2.2A). This analysis revealed that 150 transcripts (149 with FDR-adjusted $p<0.05$) showed >5-fold upregulation with CD28 costimulation 4 hours after activation. Furthermore, 699 transcripts (687 with FDR-adjusted $p<0.05$) showed >5-fold

upregulation after 24 hours. These costimulation-dependent differences could reflect either a predominately qualitative difference in the sets of genes upregulated after CD28 ligation or could simply reflect increased expression of genes already upregulated by TCR signaling. To differentiate between these possibilities, we performed Gene Set Enrichment Analysis (GSEA) (22). This technique generates ranked lists of genes that show expression differences between different activation conditions and compares this list of genes with differential expression to existing lists of genes annotated to be involved in specific cellular functions. The resulting statistical analysis is more robust at detecting biologically relevant changes in gene expression than statistical analysis of the changes of single genes. For this analysis, we focused on gene sets determined by gene ontology (GO) keywords in the Broad Institute Molecular Signatures Database (MSigDB, collection C5). At 4 hours, GSEA showed that costimulated cells have differential regulation of gene sets involved in vesicle secretion (4 GO sets with FDR q <0.6, out of 1454 sets queried; q value is the proportion of gene sets expected to be false-positives) (Supplemental table 2.1). No other gene sets reached a q value of <0.1 in this analysis. By contrast, at 24 hours, cells that received costimulation showed changes in 89 GO gene sets (FDR q<0.1). These gene sets are involved in a large variety of cellular processes, including cell cycle progression, DNA replication, and metabolism of cellular components (Supplementary Table 2.1). Thus, the differential expression of gene sets in costimulated cells shows that the qualitative effects of CD28 costimulation are very modest at 4 hours after activation and pronounced by 24 hours after activation. This difference is due to the relative transcriptional quiescence at 24 hours after activation in cells that did not receive costimulation (Figure 2.1C, upper right pane). Clustering analysis based on the global transcriptional profile showed that after 24 hours, cells activated with anti-CD3 alone have a transcriptional profile that is more similar to that of non-activated cells than to any other treatment group in the microarray analysis (Figure 2.2B). Taken together, these results show that CD28 costimulation has a small effect on the expression of a

limited number of genes at 4 hours after activation. However, by 24 hours after activation, costimulation has a profound effect on the global transcriptional profile of naive human CD4+ T cells. Cells that did not receive costimulation have a transcriptional profile similar to cells that have never been activated.

IL-2 signals do not substitute for CD28 costimulation of naive CD4+ T cells

One of the results of CD28 costimulation is the induction of IL-2 transcription. IL-2 in turn has been implicated in the production and maintenance of effector T cells, regulatory T cells, and memory T cells (23, 24). These observations raise the question of whether IL-2 signals can substitute for CD28 costimulation. To test for a role for IL-2 during T cell activation, CD4+CD45RA+ cells from three human donors were sorted and activated with anti-CD3 with or without exogenous recombinant human IL-2 (100 U/mL). As shown in Figure 2.3A, exogenous IL-2 plus TCR ligation did not increase the mean fluorescence intensity (MFI) of CD69 or CD25 to levels induced 24 hours after activation with anti-CD3 and anti-CD28. RNA from these samples was then used for real-time PCR expression analysis of 5 transcripts that were either highly up- or down-regulated by CD28 costimulation (Figure 2.3B). In none of these cases did exogenous IL-2 substitute for CD28 costimulation in modulating the expression of these genes. In an unpaired T-test, $p>0.2$ for all genes assayed comparing expression with anti-CD3 alone versus anti-CD3 + IL-2. By contrast, $p<0.05$ for CD25, TNFSF14, and BCLXL when comparing anti-CD3 versus anti-CD3+ anti-CD28; $p<0.07$ for IL2 and ZBTB20 for the same comparison.

IL-2 may not be sufficient to substitute for costimulation, but it could be necessary. To test for this possibility, CD4+CD45RA+ T cells from 3 donors were activated with anti-CD3 and anti-CD28. Before activation, CD25 (the high affinity alpha chain of the IL-2 receptor) was blocked with basiliximab, a monoclonal antibody that prevents IL-2 binding to CD25 (25). In Figure 2.3C, total blockade of CD25 is shown using a monoclonal antibody that competes for the same binding

site as BSB (clone A, fourth panel from top). However, BSB did not inhibit either CD25 or CD69 upregulation by 24 hours after activation, as measured by a non-competing fluorochrome-conjugated monoclonal antibody (clone B, Figure 2.3C bottom panel). Real-time PCR analysis of these samples from 3 donors showed that basiliximab blockade of CD25 had no consistent effect on expression of a panel of CD28-dependent transcripts 24 hours after T cell activation with CD28 costimulation (Figure 2.3D).

BHLHE40 transcription factor is required for IL-2 production and CD25 expression after activation with CD28 costimulation in Jurkat T cells

Of the transcripts that were >5-fold upregulated by CD28 costimulation at both 4 and 24 hours after activation (Table 2.1), we chose to focus on *BHLHBE40* (also referred to as DEC1, STRA13, or BHLHB2). This gene encodes a transcription factor previously shown to be important in maintaining immune homeostatsis (26); however, it has not been previously linked to CD28 costimulation. We infected Jurkat T cells with shRNA-expressing lentiviruses (with GFP to mark infected cells) targeting *BHLHBE40* transcripts or a scrambled shRNA sequence (Figure 2.4A) and confirmed knock-down of BHLHE40 mRNA (Figure 2.4B). Protein knockdown by the shRNA was confirmed in HEK-293 cells transfected with an epitope-tagged BHLHE40 (Figure 2.4C). In side-by-side cultures, the number of cells infected with the shRNA against *BHLHE40* increased much more slowly than the cells infected with control virus (Figure 2.4D). This slowed increased was due in part to greater cell death in cells with knocked-down BHLHE40 as measured by 7-AAD exclusion staining and relative loss of GFP+ cells, indicating a competitive disadvantage to cells expressing the shRNA (Figure 2.4E). The cells with diminished BHLHBE40 protein showed only 20% of the expression of IL-2 compared to control after activation with CD28 costimulation, but normal expression of CTLA-4. Likewise, the MFI of CD25 was significantly decreased in the cells with knocked-down *BHLHBE40* transcripts (Figure 2.4G), but there was no difference in CD69 upregulation after activation. In sum, this data show

that BHLHBE40 is necessary for costimulation-dependent expression of IL-2 and CD25, but is not necessary for upregulation of other markers of activation such as CTLA-4 and CD69.

BHLHBE40 is necessary for maximal transcription of CD28-dependent transcripts in primary cells

Bhlhe40 mRNA expression in naive CD4+CD45RA+ human T cells is induced by activation with CD28 costimulation (Figure 2.5A). To confirm the dependency of Bhlhe40 expression in naive mouse CD4+ T cells, we purified CD4+CD62L+CD25- cells and activated them *in vitro*. Expression of Bhlhe40 mRNA in these cells is nearly 3-fold higher with CD28 costimulation after 24 hours, compared to cells activated through the T cell receptor alone (Figure 2.5B). Thus, these data demonstrate that upregulation of Bhlhe40 after T cell activation with costimulation is evolutionarily conserved from mouse to human. To determine if BHLHE40 is important for CD28 costimulation and IL-2 production in primary cells, we purified primary CD4+ cells from *Bhlhe40* -/- and +/+ mice and activated these cells *in vitro*. Upregulation of CD69 was no different between +/+ and -/- cells (Figure 2.5C), indicating that any differences in transcription between these populations were not due to global activation differences. After 24 hours, several CD28-dependent transcripts were measured by quantitative real time PCR (Figure 2.5D). IL-2 expression in the *Bhlhe40* -/- cells was half of the +/+ cells. Bclxl levels were also decreased in the -/- cells by about 30%. There was no difference in the expression of the measured genes between +/+ and -/- cells activated with anti-CD3 alone.

BHLHBE40 heterozygosity protects from experimental autoimmune encephalitis

To confirm the functional relevance of these gene expression changes *in vivo*, *Bhlhe40* +/+ and +/- mice were immunized with MOG 35-55 peptide in Complete Freund's Adjuvant to induce experimental autoimmune encephalitis. The heterozygous mice were used rather than

homozygous mice because *Bhlhe40* -/- mice have defective circadian rhythm regulation (27), a factor that could potentially interfere with cellular immune system function (28). The average clinical scores of the +/- mice were overall lower than the +/+ controls, and 4/8 of the +/- mice were completely protected from any symptoms of EAE (a score of 0 for the entire course of experiment), whereas all +/+ controls reached a score of at least 2 (tail drooping and hind limb discoordination). The risk of developing disease for the +/- mice was significantly lower than for the +/+ mice ($p=0.018$, Fisher's exact test).

Discussion

CD28 costimulation is critical to a wide range of CD4+ T cell functions. Much of the existing literature on CD28 costimulation focuses on membrane-proximal signaling events. In this study, we focused on the transcriptional effects of CD28 costimulation. Using microarray expression analysis, we defined a transcriptional profile for CD28 costimulation in primary human naive CD4+ T cells and identify a transcription factor, Bhlhe40, that is upregulated with CD28 costimulation and is necessary for maximal transcription of IL-2 and Bclxl, two highly CD28-dependent genes. Further, we show that Bhlhe40 is necessary for maximal disease in experimental autoimmune encephalitis in the mouse, a CD28-dependent disease (29-31).

Our microarray analysis of activated CD4+ T cells showed that CD28 ligation has different effects on global transcriptional profile at different times after initial activation. In particular, CD28 costimulation induces primarily quantitative changes in gene transcription for the first several hours after T cell activation via the T cell receptor. Any qualitative differences in gene expression at this early time point are limited to a small set of genes, most prominently IL-2. However, by 24 hours after activation, the effects of CD28 costimulation are mostly qualitative. In fact, the transcriptional profile of a T cell that received TCR signals alone is similar to that of a T cell that was never activated. These data are in contrast to previous studies (17)(18) that have shown that the CD28 signal provides a mostly quantitative boost to the gene transcription profile induced by T cell receptor ligation (4). Gene set enrichment analysis of CD28-dependent genes 24 hours after activation confirmed previous work showing that CD28 signals regulate genes involved in cellular metabolism and cell cycle progression (18)(32). At 4 hours after activation, our analysis revealed that all CD28-dependent gene sets were involved in vesicle transport processes. This result raises the possibility that a critical early qualitative effect CD28 costimulation is the induction and assembly of cytokine secretion machinery in the T cell.

Importantly, in the current study, we separated naive CD4+CD45RA+ T cells for all human T cell activation experiments. We titrated antibody concentrations to deliver maximal TCR signals and we minimized variability among human donors selected for microarray analysis. Previous studies argued primarily for a quantitative effect of CD28 costimulation on the global transcriptional profile of activated T cells. However, interpretation of the data from these studies is complicated by the use of mixed populations of cells with varying requirements for CD28 costimulation: either unfractionated primary human T cells (18) or whole primary human CD4+ T cells (17).

In an attempt to define a mechanism for the observed effects of CD28 costimulation, we show that exogenous IL-2 could not substitute for CD28 costimulation in promoting transcription of a panel of CD28-dependent genes. Further, basiliximab blocking of CD25, the high affinity IL-2 receptor, did not interfere with the transcriptional effects of CD28 costimulation, shown by expression of a panel of CD28-dependent transcripts. Taken together, these data imply that a cell-intrinsic mechanism and not IL-2 cytokine feedback drives transcriptional changes induced by 24 hours after T cell activation with CD28 costimulation.

What transcription factors might be responsible for the unique transcriptional response to CD28 costimulation? Recent work has shown that CD28-dependent PDK1 and PKC-theta recruitment drives NF-kappaB activation (33)(34), which might be responsible for CD28-dependent phenotypes, such as IL-2 production. The transcription factor c-Rel is critical for IL-2 production and T cell proliferation along with a variety of other NF-kappaB family members (35)(36)(37)(38)(39). Although NF-kappaB family members are critical for T cell development and cytokine production, we set out to find transcription factors whose function was more narrowly limited to directing the transcriptional response to CD28 costimulation in fully differentiated naive CD4+ T cells. To generate candidates, we used microarray data to generate a list of genes that were more than 5-fold upregulated by CD28 costimulation at both the 4 hour

and 24 hour time points. From this list, we chose to focus on Bhlhe40 (also known as DEC1, Stra13, BHLHB2, and Clast5), a basic-helix-loop-helix transcription factor involved in a wide variety of biological processes including regulating circadian rhythms (40), repressing brain-derived neurotrophic factor transcription in cultured neurons (41), and responding to hypoxic stress(42, 43)(44). Importantly, Bhlhe40 is highly expressed in resting B cells and is rapidly down-regulated upon B cell activation (45). Transgenic expression of Bhlhe40 in primary mouse B cells decreases both B cell numbers and B cell proliferation after activation (45)(46). We knocked down Bhlhe40 in Jurkat T cells to test for any effects on CD28 costimulation. Strikingly, Jurkat cells with knocked-down Bhlhe40 showed normal upregulation of CD69, but decreased surface CD25 protein and IL-2 mRNA levels after activation with CD28. The normal induction of CD69 indicates that loss of Bhlhe40 expression does not globally depress T cell activation, but rather specifically affects CD28-dependent gene expression.

The original publication describing the BHLHE40 null mouse (26) reported that after 6-8 months, about 80% of null females and 50% of null males showed grossly enlarged spleen and lymph nodes with large numbers of activated T and B cells in secondary lymphoid organs (26). In addition, *Bhlhe40 -/-* CD4+ T cells produced less IL-2 upon stimulation than control cells (26). Because CD28 costimulation is critical for regulatory T cell production and homeostasis (47,48, 49), this result suggests that the observed phenotype of this mouse might be due to defects in CD28 costimulation. All of the reported phenotypes of the Bhlhe40-deficient T cells could be potentially linked to the deficit in IL-2 production, because IL-2 is an important growth factor for both regulatory T cells and effector T cells (50). In our hands, these mice did not develop lymphoproliferative disease when aged for over a year (data not shown).

No spontaneous autoimmunity has been reported for an independent Bhlhe40 gene-disrupted mouse (41). In our hands, no differences in percentages of early thymic progenitors or CD4+/8+ double-positive or single-positive T cell numbers were observed in the thymi of these

Bhlhe40 -/- mice, compared to control mice (data not shown). A statistically significant higher percentage of memory CD8+ T cells (CD44+CD62L+) were found in the spleens of *Bhlhe40 -/-* animals (25%) compared to control animals (18%). However, there was no difference in the percentage of effector, memory, or naive CD4+ T cells in the spleen between *Bhlhe40 -/-* and +/+ mice. Thus, the development and peripheral homeostasis of CD4+ T cells appears to be intact in *Bhlhe40 -/-* animals.

Using the *Bhlhe40*-null mice (41), we show that the expression of a panel of costimulation-dependent genes is decreased in *Bhlhe40 -/-* CD4+ T cells compared to +/+ controls after activation with anti-CD3 and anti-CD28. In particular, IL-2 expression was decreased by about 50% in the *Bhlhe40*-null cells. By contrast, there is no significant difference in the expression of Il2, Nr4a3, Ifng, or Bclxl in *Bhlhe40*-null CD4+ cells compared to control cells after stimulation with anti-CD3 alone. These results show the specificity of the effect of loss of Bhlhe40 on CD28 costimulation. Nevertheless, loss of Bhlhe40 does not completely block the transcriptional response to costimulation, implying that there may be some partial compensation by other transcription factors.

To test for an *in vivo* role for Bhlhe40 in immune system function, we induced experimental autoimmune encephalitis in *Bhlhe40* +/+ and +/- animals. The +/- animals were partially protected from disease. Thus, the observed defects of *in vitro* cytokine production after activation correlate with a reduced risk of developing EAE, a highly costimulation-dependent disease (29-31).

Importantly, Bhlhe40 has a closely related homolog named Bhlhe41 which shares 100% protein sequence identity in the basic helix-loop-helix DNA binding domain. Bhlhe41 has recently been shown to be necessary for Th2 differentiation, IL-2 production, and CD25 expression in primary mouse T cells (51, 52). Thus, it is possible that Bhlhe40 and Bhlhe41

synergize to drive costimulation-dependent phenotypes. These two genes have been previously shown to work together to regulator mammalian circadian rhythms (40). Further work is now underway to determine whether these transcription factors also collaborate to direct transcription of CD28-dependent genes in CD4+ T cells.

Materials and methods

Human blood

Whole blood was obtained via venipuncture from healthy adult volunteers (males, age range 19-29). These volunteers did not report any autoimmune disorders or symptoms of respiratory viral infection. Informed consent was obtained in accordance with UCSF approved policies and procedures. Blood was collected in sodium heparin-containing Vacutainer tubes (Becton Dickinson [BD], Franklin Lakes, NJ). Peripheral blood mononuclear cells were isolated by using Ficoll-Paque PLUS (Amersham Biosciences, Uppsala Sweden), as previously described (53).

Isolation and activation of human CD4+CD45RA+ T cells

For microarray analysis, CD4+CD45RA+ T cells were isolated on a BD FACSAria II cell sorter (BD Biosciences, San Jose, CA) with the following antibodies: PerCP-conjugated anti-CD4 (BD, clone SK3) and FITC-conjugated CD45RA (BD, clone HI100). Purity of the sorted population was >99%. These cells were then seeded into wells of a 12-well plate at a density of $1x10^6$ cells per mL of RMPI-1640 supplemented with 5% human heat-inactivated pooled AB serum (Valley Biomedical, Winchester, VA). The cells were activated with latex beads conjugated to control antibody (BD, clone MPC-11) or antibodies specific for anti-CD3 (clone OKT3) or to both anti-CD3 and anti-CD28 (clone 9.3). Activation was confirmed by staining with anti-CD25 (BD, clone 2A3) and anti-CD69 (BD, clone L78), and analysis by flow cytometry on a BD Biosciences FACSCalibur. For other *in vitro* experiments with human T cells, PBMC were isolated as above, and CD4+CD45RA+ cells were isolated with a RoboSep (Stem Cell Technologies, Vancouver, Canada) and the human naive T cell enrichment kit (Stem Cell, Vancouver, Canada). This method consistently gave purities of >90% CD4+CD45RA+ cells. The cells were then activated on 12-well plates seeded the previous night with anti-CD3 or anti-CD3 and anti-CD28 at 1 ug/mL (anti-CD3) or 10 ug/mL (anti-CD28) in PBS. The plates were then washed 3x in PBS before cells were added in RPMI-1640 with 5% FCS. Basiliximab (BSB, Simulect, Novartis Pharmaceuticals)

was a gift from Dr. Flavio Vincenti. Confirmation of basiliximab blocking of CD25 was performed with a competing monoclonal anirobody labeled "A" (BD clone 2A3) and a non-competing monoclonal antibody labeled "B" (BD clone MA251). The concentration of basiliximab was 25 ug/mL. Recombinant human interleukin-2 (Proleukin; Chiron Therapeutics, Emeryville, CA) was added at 100 units/ml.

RNA preparation and microarray analysis

RNA samples for microarray were prepared via Trizol extraction and the quantity, purity, and integrity of the samples were measured with a Nanodrop and a Bioanalyzer. The samples were then reverse transcribed and amplified before hybridization to Affymetrix human U133 Plus 2 microarrays. Hybridization and data collection were performed by the Genome Core of the The J. David Gladstone Institutes. RNA samples for quantitative real-time PCR analysis were extracted using the RNAeasy kit (Qiagen, Valencia CA) using the manufacturer's recommended protocol.

Microarray data analysis

Microarray image files were visually inspected by using the BioConductor package for R. Files with visible artifacts were excluded from the analysis. Data were normalized by using Genespring GX 10.0.2 software (Agilent Technologies, Santa Clara CA) with GCRMA. Statistical significance of differential expression was calculated using ANOVA followed by Benjamini Hochberg FDR (false discovery rate), with a cut-off of $p<0.05$. Gene set enrichment analysis (GSEA) was performed with Genespring GX 10.0.2 software. The minimum number of matching genes was set at 15 and the limit of permutations was set at 100. All gene sets reported have a FDR $q< 0.1$. Clustering analysis was also performed with Genespring software, using all probes in the dataset. Distance metric was set to Euclidean and the linkage rule was set to average.

Quantitative real-time PCR

Reverse transcription of RNA samples and quantitative real-time PCR was done as previously described (54). Taqman primer probes (Applied Biosystems, Foster City, CA) used were: IL-2 (Hs99999150_m1), BHLHE40 (Hs00186419_m1), CD25 (Hs00907777_m1), BCLXL (Hs99999146_m1), NR4A3 (Hs00545009_g1), SGPP2 (Hs00544786_m1), TNFRSF9 (Hs00155512_m1), TNFRSF14 (Hs00542476_g1), UHRF1 (Hs00273589_m1), and ZBTB20 (Hs00210321_m1).

DNA cloning and lentivirus production

Lentivirus encoding an shRNA specific for hBHLHE40 (pSICO-R-502) was produced by using the pSICO-R vector. Empty vectors were cut with XhoI and HpaI. The following primers were then annealed and ligated into the cut vector, forward: TGCATGTGAAAGCACTAACATTCAAGAGATGTTAGTGCTTTCACATGCTTTTTTC and reverse: TCGAGAAAAAAGCATGTGAAAGCACTAACATCTCTTGAATGTTAGTGCTTTCACATG CA. The for the control scrambled shRNA (pSICO-R-SCRM), the following primers were used, forward: TTCATCGAGTATTATTCCTATTCAAGAGATAGGAATAATACTCGATGATTTTTTC; reverse: TCGAGAAAAAATCATCGAGTATTATTCCTATCTCTTGAATAGGAATAATACTCGATG AA. Lentivirus was produced in HEK 293 cells, using psPAX2 and pCMV-VSV-G. Jurkat T cells were infected by mixing viral supernatant with Jurkat cells resuspended in RPMI-1640 + 5% FCS at a concentration of $1x10^6$ per mL.

Jurkat activation

Jurkat T cells (a gift from Dr. Jeroen Roose) were infected with pSICO-R lentivirus by mixing viral supernatant with Jurkat cells resuspended in RMPI-1640 5% FBS at a 1:1 ratio. After 48 hours, productive infection was confirmed by GPF expression. The Jurkat cells were activated with plate-bound anti-CD3 (clone OKT3) or anti-CD3 and anti-CD28 (clone 9.3). One ug/mL of anti-CD3 with or without 10 ug/mL anti-CD28 in PBS was put into wells of 12- or 6- well plates. The next day, the wells were washed 3 times with PBS and Jurkat cells were seeded at a density of $1x10^6$ cells per mL of RPMI-1640 supplemented with 5% FCS, glutamine, penicillin, and streptomycin. Cell surface staining with fluorochrome-conjugated antibodies was done as detailed above for primary human cells. Dead cells were excluded by staining with 7-aminoactinomycin D (BD, San Jose CA), according to the manufacturer's instructions.

Western blot analysis

HEK 293 cells were co-transfected with Lipofectamine 2000 (Invitrogen) with endotoxin-free preparations of pN1-eGFP-2A-BHLHE40 and either pSICO-R-502 or pSICO-R expressing a scrambled shRNA, according to the manufacturer's instructions. Whole cell extracts were prepared in RIPA buffer (1% Triton X-100, 150 mM NaCl, 1 mM Tris pH 8.0, 1 mM EDTA, 0.5M 5% glycerol, 0.1% sodium deoxycholate, 0.1% SDS) supplemented with DNAseI and 10 mM $CaCl_2$. Protein concentration in each sample was determined with a BCA protein assay kit (Thermo Scientific/Pierce, Rockford, IL). From each sample, 40 ug of whole cell extract was boiled for 10 minutes in Laemmli buffer with dithiothreitol added to 0.2 M. The samples were run on a NOVEX-NuPAGE 10% Bis/Tris minigel (Invitrogen). The gel was transferred to a PVDF membrane (BioRad, Hercules, CA), blocked in TBST (100 mM Tris pH 7.5, 0.9% NaCl, 0.1% v/v Tween-20) and 5% nonfat milk overnight. The membrane was then incubated with HRP-conjugated anti-6xHIS monoclonal antibody (BD, clone F24-796) for 5 hours. The membrane was washed 5 times in TBST for 5 minutes each, and washed for a final time for 10 minutes in

TBS. The blot was developed with Supersignal West Pico Chemiluminescent Substrate (Thermo Scientific/Pierce, Rockford, IL).

Mice

Bhlhe40 -/- mice on a mixed genetic background (129, C57BL/6, and CD1) or on a pure C57BL/6 background (from the Jackson Laboratory) were all derived from the mouse line described in (41). Mice were bred and housed in a specific pathogen-free barrier facility at the University of California, San Francisco or at the National Institute on Aging at the Johns Hopkins Bayview Campus in Baltimore, MD. All animal experiments were approved by the University of California, San Francisco, Animal Care and Use Committee. For activation assays, CD4+ T cells were purified from lymph nodes and spleens with a RoboSep (StemCell Technologies, Vancouver BC) and the StemCell mouse CD4+ T cell enrichment kit. Cell purities were typically >90% CD4+. Alternatively, CD4+CD25-CD62L+ cells were sorted on a Moflo flow cytometer using FITC-conjugated anti-CD4 (clone GK1.5, Southern Biotech, Birmingham, AL), PE-conjugated anti-CD25 (clone PC61, BD Biosciences, San Jose, CA), and Alexa647-conjugatred CD62L (clone MEL-14, UCSF Monoclonal Antibody Core) . For *in vitro* activation experiments, cells were resuspended in DMEM supplemented with 10% FBS, glutamine, HEPES buffer, 0.1% β-mercaptoethanol, non-essential amino acids, and antibiotics. The cells were activated in plates pre-coated with 1 μg/mL anti-CD3 (clone 145-2C11) and 1 μg/mL anti-CD28 (clone PV1).

EAE

Experimental autoimmune encephalitis was induced by injecting 200 ug of MOG 35-55 peptide (Genemed Synthesis, San Antonio TX) emulsified in CFA (Sigma, St. Louis MO) subcutaneously at three locations on the back of each mouse. Intraperitoneal injection of pertussis toxin (400 ng per dose, List Biological Labs, Campbell CA) was administered to each mouse on the day of

immunization and on day 2 after immunization. Clinical scores were assessed every two days, according to the following criteria: 1, weak tail or weak hind limb; 2 weak tail and weak hind limb; 3 partial hind limb paralysis; 4 complete hindlimb paralysis; 5, moribund.

Acknowledgements

We thank Weihong Lui, Amy Putnam, and David Gumbiner for assistance with human blood collection and processing. We thank Dr. Christopher S. Barker of the Genomics Core of the J. David Gladstone Institutes for assistance with the microarray experiments. We thank Mike Lee and Shuwei Zhang for assistance with cell sorting. We thank Mark P. Mattson for providing some *Bhlhe40 -/- mice*. This work was supported by NIH grant P01 AI35297.

References

1. Lenschow, D. J., T. L. Walunas, and J. A. Bluestone. 1996. CD28/B7 system of T cell costimulation. *Annu. Rev. Immunol.* 14: 233-258.

2. Schwartz, R. H. 2003. T cell anergy. *Annu. Rev. Immunol.* 21: 305-334.

3. Macian, F., S. H. Im, F. J. Garcia-Cozar, and A. Rao. 2004. T-cell anergy. *Curr. Opin. Immunol.* 16: 209-216.

4. Acuto, O. and F. Michel. 2003. CD28-mediated co-stimulation: a quantitative support for TCR signalling. *Nat. Rev. Immunol.* 3: 939-951.

5. Acuto, O., S. Mise-Omata, G. Mangino, and F. Michel. 2003. Molecular modifiers of T cell antigen receptor triggering threshold: the mechanism of CD28 costimulatory receptor. *Immunol. Rev.* 192: 21-31.

6. Yokosuka, T., W. Kobayashi, K. Sakata-Sogawa, M. Takamatsu, A. Hashimoto-Tane, M. L. Dustin, M. Tokunaga, and T. Saito. 2008. Spatiotemporal regulation of T cell costimulation by TCR-CD28 microclusters and protein kinase C theta translocation. *Immunity* 29: 589-601.

7. Kane, L. P., P. G. Andres, K. C. Howland, A. K. Abbas, and A. Weiss. 2001. Akt provides the CD28 costimulatory signal for up-regulation of IL-2 and IFN-gamma but not TH2 cytokines. *Nat. Immunol.* 2: 37-44.

8. Rudd, C. E. and M. Raab. 2003. Independent CD28 signaling via VAV and SLP-76: a model for in trans costimulation. *Immunol. Rev.* 192: 32-41.

9. Michel, F., G. Mangino, G. Attal-Bonnefoy, L. Tuosto, A. Alcover, A. Roumier, D. Olive, and O. Acuto. 2000. CD28 utilizes Vav-1 to enhance TCR-proximal signaling and NF-AT activation. *J. Immunol.* 165: 3820-3829.

10. Tavano, R., R. L. Contento, S. J. Baranda, M. Soligo, L. Tuosto, S. Manes, and A. Viola. 2006. CD28 interaction with filamin-A controls lipid raft accumulation at the T-cell immunological synapse. *Nat. Cell Biol.* 8: 1270-1276.

11. Macian, F., F. Garcia-Cozar, S. H. Im, H. F. Horton, M. C. Byrne, and A. Rao. 2002. Transcriptional mechanisms underlying lymphocyte tolerance. *Cell* 109: 719-731.

12. Pan, M., M. M. Winslow, L. Chen, A. Kuo, D. Felsher, and G. R. Crabtree. 2007. Enhanced NFATc1 nuclear occupancy causes T cell activation independent of CD28 costimulation. *J. Immunol.* 178: 4315-4321.

13. Zhang, J., T. Bardos, D. Li, I. Gal, C. Vermes, J. Xu, K. Mikecz, A. Finnegan, S. Lipkowitz, and T. T. Glant. 2002. Cutting edge: regulation of T cell activation threshold by CD28 costimulation through targeting Cbl-b for ubiquitination. *J. Immunol.* 169: 2236-2240.

14. Shan, X., M. J. Czar, S. C. Bunnell, P. Liu, Y. Liu, P. L. Schwartzberg, and R. L. Wange. 2000. Deficiency of PTEN in Jurkat T cells causes constitutive localization of Itk to the plasma membrane and hyperresponsiveness to CD3 stimulation. *Mol. Cell. Biol.* 20: 6945-6957.

15. Croft, M., L. M. Bradley, and S. L. Swain. 1994. Naive versus memory CD4 T cell response to antigen. Memory cells are less dependent on accessory cell costimulation and can respond to many antigen-presenting cell types including resting B cells. *J. Immunol.* 152: 2675-2685.

16. Dubey, C., M. Croft, and S. L. Swain. 1996. Naive and effector CD4 T cells differ in their requirements for T cell receptor versus costimulatory signals. *J. Immunol.* 157: 3280-3289.

17. Riley, J. L., M. Mao, S. Kobayashi, M. Biery, J. Burchard, G. Cavet, B. P. Gregson, C. H. June, and P. S. Linsley. 2002. Modulation of TCR-induced transcriptional profiles by ligation of CD28, ICOS, and CTLA-4 receptors. *Proc. Natl. Acad. Sci. U. S. A.* 99: 11790-11795.

18. Diehn, M., A. A. Alizadeh, O. J. Rando, C. L. Liu, K. Stankunas, D. Botstein, G. R. Crabtree, and P. O. Brown. 2002. Genomic expression programs and the integration of the CD28 costimulatory signal in T cell activation. *Proc. Natl. Acad. Sci. U. S. A.* 99: 11796-11801.

19. Amyes, E., A. J. McMichael, and M. F. Callan. 2005. Human CD4+ T cells are predominantly distributed among six phenotypically and functionally distinct subsets. *J. Immunol.* 175: 5765-5773.

20. Radich, J. P., M. Mao, S. Stepaniants, M. Biery, J. Castle, T. Ward, G. Schimmack, S. Kobayashi, M. Carleton, J. Lampe, and P. S. Linsley. 2004. Individual-specific variation of gene expression in peripheral blood leukocytes. *Genomics* 83: 980-988.

21. Whitney, A. R., M. Diehn, S. J. Popper, A. A. Alizadeh, J. C. Boldrick, D. A. Relman, and P. O. Brown. 2003. Individuality and variation in gene expression patterns in human blood. *Proc. Natl. Acad. Sci. U. S. A.* 100: 1896-1901.

22. Subramanian, A., P. Tamayo, V. K. Mootha, S. Mukherjee, B. L. Ebert, M. A. Gillette, A. Paulovich, S. L. Pomeroy, T. R. Golub, E. S. Lander, and J. P. Mesirov. 2005. Gene set enrichment analysis: a knowledge-based approach for interpreting genome-wide expression profiles. *Proc. Natl. Acad. Sci. U. S. A.* 102: 15545-15550.

23. Dooms, H. and A. K. Abbas. 2006. Control of CD4+ T-cell memory by cytokines and costimulators. *Immunol. Rev.* 211: 23-38.

24. Lohr, J., B. Knoechel, and A. K. Abbas. 2006. Regulatory T cells in the periphery. *Immunol. Rev.* 212: 149-162.

25. Binder, M., F. N. Vogtle, S. Michelfelder, F. Muller, G. Illerhaus, S. Sundararajan, R. Mertelsmann, and M. Trepel. 2007. Identification of their epitope reveals the structural basis for the mechanism of action of the immunosuppressive antibodies basiliximab and daclizumab. *Cancer Res.* 67: 3518-3523.

26. Sun, H., B. Lu, R. Q. Li, R. A. Flavell, and R. Taneja. 2001. Defective T cell activation and autoimmune disorder in Stra13-deficient mice. *Nat. Immunol.* 2: 1040-1047.

27. Rossner, M. J., H. Oster, S. P. Wichert, L. Reinecke, M. C. Wehr, J. Reinecke, G. Eichele, R. Taneja, and K. A. Nave. 2008. Disturbed clockwork resetting in Sharp-1 and Sharp-2 single and double mutant mice. *PLoS One* 3: e2762.

28. Pownall, R., P. A. Kabler, and M. S. Knapp. 1979. The time of day of antigen encounter influences the magnitude of the immune response. *Clin. Exp. Immunol.* 36: 347-354.

29. Perrin, P. J., C. H. June, J. H. Maldonado, R. B. Ratts, and M. K. Racke. 1999. Blockade of CD28 during in vitro activation of encephalitogenic T cells or after disease onset ameliorates experimental autoimmune encephalomyelitis. *J. Immunol.* 163: 1704-1710.

30. Perrin, P. J., D. Scott, L. Quigley, P. S. Albert, O. Feder, G. S. Gray, R. Abe, C. H. June, and M. K. Racke. 1995. Role of B7:CD28/CTLA-4 in the induction of chronic relapsing experimental allergic encephalomyelitis. *J. Immunol.* 154: 1481-1490.

31. Oliveira-dos-Santos, A. J., A. Ho, Y. Tada, J. J. Lafaille, S. Tonegawa, T. W. Mak, and J. M. Penninger. 1999. CD28 costimulation is crucial for the development of spontaneous autoimmune encephalomyelitis. *J. Immunol.* 162: 4490-4495.

32. Frauwirth, K. A., J. L. Riley, M. H. Harris, R. V. Parry, J. C. Rathmell, D. R. Plas, R. L. Elstrom, C. H. June, and C. B. Thompson. 2002. The CD28 signaling pathway regulates glucose metabolism. *Immunity* 16: 769-777.

33. Park, S. G., J. Schulze-Luehrman, M. S. Hayden, N. Hashimoto, W. Ogawa, M. Kasuga, and S. Ghosh. 2009. The kinase PDK1 integrates T cell antigen receptor and CD28 coreceptor signaling to induce NF-kappaB and activate T cells. *Nat. Immunol.* 10: 158-166.

34. Takeda, K., Y. Harada, R. Watanabe, Y. Inutake, S. Ogawa, K. Onuki, S. Kagaya, K. Tanabe, H. Kishimoto, and R. Abe. 2008. CD28 stimulation triggers NF-kappaB activation through the CARMA1-PKCtheta-Grb2/Gads axis. *Int. Immunol.* 20: 1507-1515.

35. Rao, S., S. Gerondakis, D. Woltring, and M. F. Shannon. 2003. c-Rel is required for chromatin remodeling across the IL-2 gene promoter. *J. Immunol.* 170: 3724-3731.

36. Sanchez-Valdepenas, C., A. G. Martin, P. Ramakrishnan, D. Wallach, and M. Fresno. 2006. NF-kappaB-inducing kinase is involved in the activation of the CD28 responsive element through phosphorylation of c-Rel and regulation of its transactivating activity. *J. Immunol.* 176: 4666-4674.

37. Marinari, B., A. Costanzo, V. Marzano, E. Piccolella, and L. Tuosto. 2004. CD28 delivers a unique signal leading to the selective recruitment of RelA and p52 NF-kappaB subunits on IL-8 and Bcl-xL gene promoters. *Proc. Natl. Acad. Sci. U. S. A.* 101: 6098-6103.

38. Kempiak, S. J., T. S. Hiura, and A. E. Nel. 1999. The Jun kinase cascade is responsible for activating the CD28 response element of the IL-2 promoter: proof of cross-talk with the I kappa B kinase cascade. *J. Immunol.* 162: 3176-3187.

39. Kontgen, F., R. J. Grumont, A. Strasser, D. Metcalf, R. Li, D. Tarlinton, and S. Gerondakis. 1995. Mice lacking the c-rel proto-oncogene exhibit defects in lymphocyte proliferation, humoral immunity, and interleukin-2 expression. *Genes Dev.* 9: 1965-1977.

40. Honma, S., T. Kawamoto, Y. Takagi, K. Fujimoto, F. Sato, M. Noshiro, Y. Kato, and K. Honma. 2002. Dec1 and Dec2 are regulators of the mammalian molecular clock. *Nature* 419: 841-844.

41. Jiang, X., F. Tian, Y. Du, N. G. Copeland, N. A. Jenkins, L. Tessarollo, X. Wu, H. Pan, X. Z. Hu, K. Xu, H. Kenney, S. E. Egan, H. Turley, A. L. Harris, A. M. Marini, and R. H. Lipsky. 2008. BHLHB2 controls Bdnf promoter 4 activity and neuronal excitability. *J. Neurosci.* 28: 1118-1130.

42. Ivanov, S. V., K. Salnikow, A. V. Ivanova, L. Bai, and M. I. Lerman. 2007. Hypoxic repression of STAT1 and its downstream genes by a pVHL/HIF-1 target DEC1/STRA13. *Oncogene* 26: 802-812.

43. Ivanova, A. V., S. V. Ivanov, A. Danilkovitch-Miagkova, and M. I. Lerman. 2001. Regulation of STRA13 by the von Hippel-Lindau tumor suppressor protein, hypoxia, and the UBC9/ubiquitin proteasome degradation pathway. *J. Biol. Chem.* 276: 15306-15315.

44. Miyazaki, K., T. Kawamoto, K. Tanimoto, M. Nishiyama, H. Honda, and Y. Kato. 2002. Identification of functional hypoxia response elements in the promoter region of the DEC1 and DEC2 genes. *J. Biol. Chem.* 277: 47014-47021.

45. Seimiya, M., R. Bahar, Y. Wang, K. Kawamura, Y. Tada, S. Okada, M. Hatano, T. Tokuhisa, H. Saisho, T. Watanabe, M. Tagawa, and J. O-Wang. 2002. Clast5/Stra13 is a negative regulator of B lymphocyte activation. *Biochem. Biophys. Res. Commun.* 292: 121-127.

46. Seimiya, M., A. Wada, K. Kawamura, A. Sakamoto, Y. Ohkubo, S. Okada, M. Hatano, T. Tokuhisa, T. Watanabe, H. Saisho, M. Tagawa, and J. O-Wang. 2004. Impaired lymphocyte development and function in Clast5/Stra13/DEC1-transgenic mice. *Eur. J. Immunol.* 34: 1322-1332.

47. Vang, K. B., J. Yang, A. J. Pagan, L. X. Li, J. Wang, J. M. Green, A. A. Beg, and M. A. Farrar. 2010. Cutting edge: CD28 and c-Rel-dependent pathways initiate regulatory T cell development. *J. Immunol.* 184: 4074-4077.

48. Salomon, B., D. J. Lenschow, L. Rhee, N. Ashourian, B. Singh, A. Sharpe, and J. A. Bluestone. 2000. B7/CD28 costimulation is essential for the homeostasis of the CD4+CD25+ immunoregulatory T cells that control autoimmune diabetes. *Immunity* 12: 431-440.

49. Bour-Jordan, H., B. L. Salomon, H. L. Thompson, G. L. Szot, M. R. Bernhard, and J. A. Bluestone. 2004. Costimulation controls diabetes by altering the balance of pathogenic and regulatory T cells. *J. Clin. Invest.* 114: 979-987.

50. Hoyer, K. K., H. Dooms, L. Barron, and A. K. Abbas. 2008. Interleukin-2 in the development and control of inflammatory disease. *Immunol. Rev.* 226: 19-28.

51. Liu, Z., Z. Li, K. Mao, J. Zou, Y. Wang, Z. Tao, G. Lin, L. Tian, Y. Ji, X. Wu, X. Zhu, S. Sun, W. Chen, C. Xiang, and B. Sun. 2009. Dec2 promotes Th2 cell differentiation by enhancing IL-2R signaling. *J. Immunol.* 183: 6320-6329.

52. Yang, X. O., P. Angkasekwinai, J. Zhu, J. Peng, Z. Liu, R. Nurieva, X. Liu, Y. Chung, S. H. Chang, B. Sun, and C. Dong. 2009. Requirement for the basic helix-loop-helix transcription factor Dec2 in initial TH2 lineage commitment. *Nat. Immunol.* 10: 1260-1266.

53. Putnam, A. L., T. M. Brusko, M. R. Lee, W. Liu, G. L. Szot, T. Ghosh, M. A. Atkinson, and J. A. Bluestone. 2009. Expansion of human regulatory T-cells from patients with type 1 diabetes. *Diabetes* 58: 652-662.

54. Esensten, J. H., M. R. Lee, L. H. Glimcher, and J. A. Bluestone. 2009. T-bet-deficient NOD mice are protected from diabetes due to defects in both T cell and innate immune system function. *J. Immunol.* 183: 75-82.

Figures

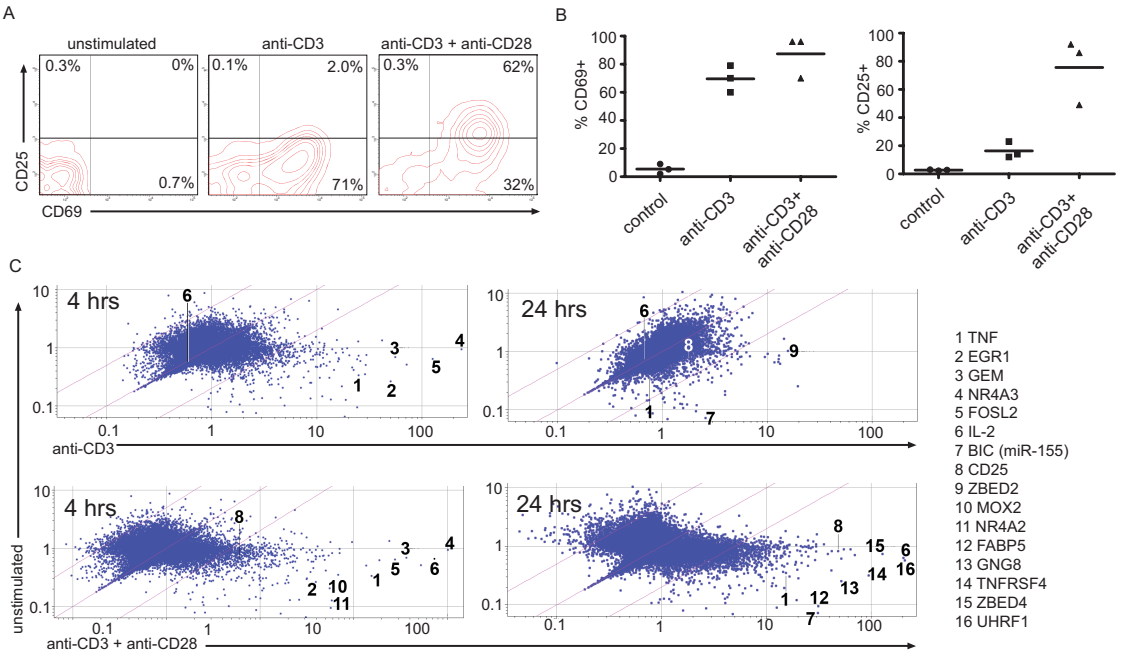

Figure 2.1. **Profile of CD28 costimulation-dependent transcription.**

A, Primary human CD4+CD45RA+ cells (naive T cells) were isolated and activated *in vitro* with anti-CD3 or anti-CD3 and anti-CD28 for 24 hours before flow cytometry analysis. Data are from one of 7 independent donors. B, Quantitation of activation as measured by mean fluorescence intensity (MFI) of CD69 and CD25 from 3 donors used in the microarray experiments. C, RNA from cells activated with anti-CD3 or anti-CD3 and anti-CD28 were harvested at 4 hours (top panel) or 24 hours (bottom panel) after activation and microarray analysis was performed. The resulting expression data were graphed as a scatter plot, with 16 highly CD28-inducible genes labeled according to the list at right.

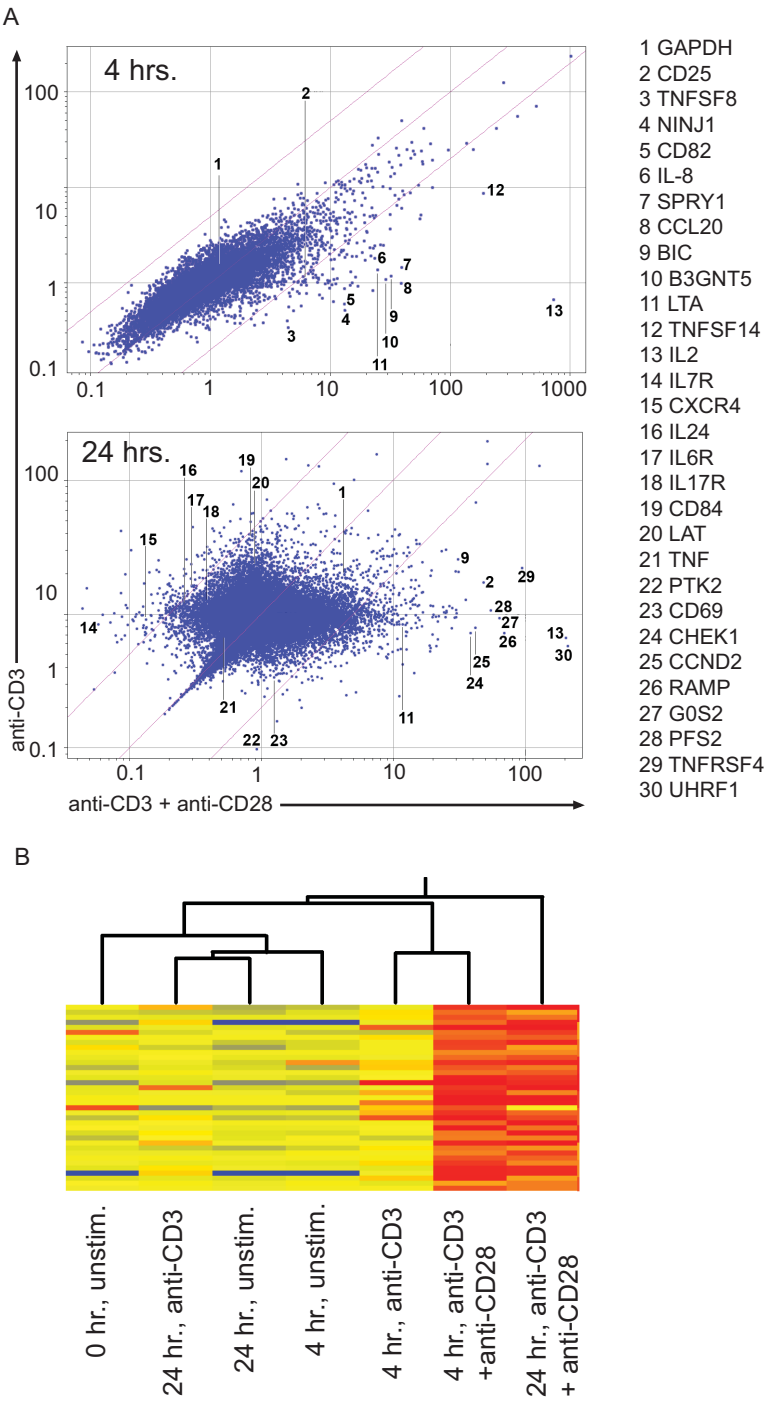

Figure 2.2. **Costimulation is required to maintain the transcriptional profile of activation.** A, Microarray data described in Figure 1 were graphed to show a scatter plot of expression values of the samples activated with anti-CD3 versus the samples activated with anti-CD3 and anti-CD28, at both 4 and 24 hours after activation. A list of notable or differentially expressed genes is at right. B, Clustering of treatment groups based on global transcriptional profile. The probes shown are from genes in Table 2.1. Red transcripts are upregulated, yellow transcripts are unchanged, and blue transcripts are downregulated.

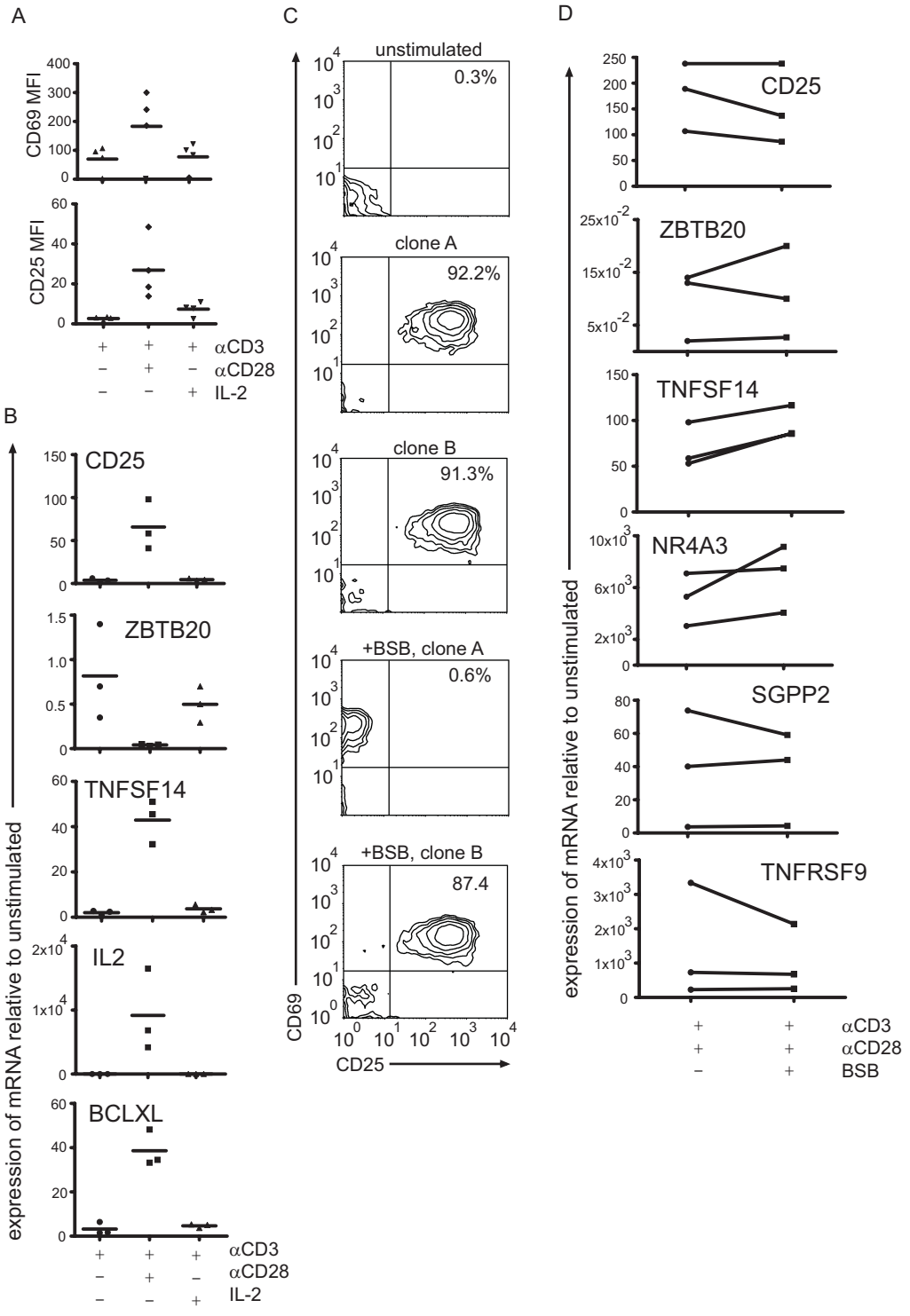

Figure 2.3. **IL-2 autocrine feedback cannot substitute for CD28 costimulation.** A, Primary human CD4+CD45RA+ T cells from three donors were activated *in vitro* for 24 hours as

indicated with or without 100 U/mL recombinant human interleukin-2. Cells were harvested and stained for CD69 and CD25 activation markers and analyzed by flow cytometry. B, RNA was harvested 24 hours after activation from the cells in panel A. Quantitative real-time PCR was used to measure the levels of the indicated transcripts, normalized to both the 18S rRNA and to the level of the indicated transcript in resting cells. C, Primary human CD4+CD45RA+ T cells were activated *in vitro* as indicated in the presences of basiliximab (BSB, 25 ug/mL). After 24 hours, the cells were then stained with fluorochrome-conjugated anti-CD25. Monoclonal antibody A binds competitively with BSB and monoclonal antibody B binds non-competitively. Results shown are representative of three independent experiments. D, RNA was harvested from samples in part C and control samples that were not treated with BSB. Quantitative real-time PCR was used to measure the levels of the indicated transcripts. The data were normalized to both the 18S rRNA and to the level of the indicated transcript in unstimulated cells. Lines connect samples from the same donor. Results are from three independent experiments.

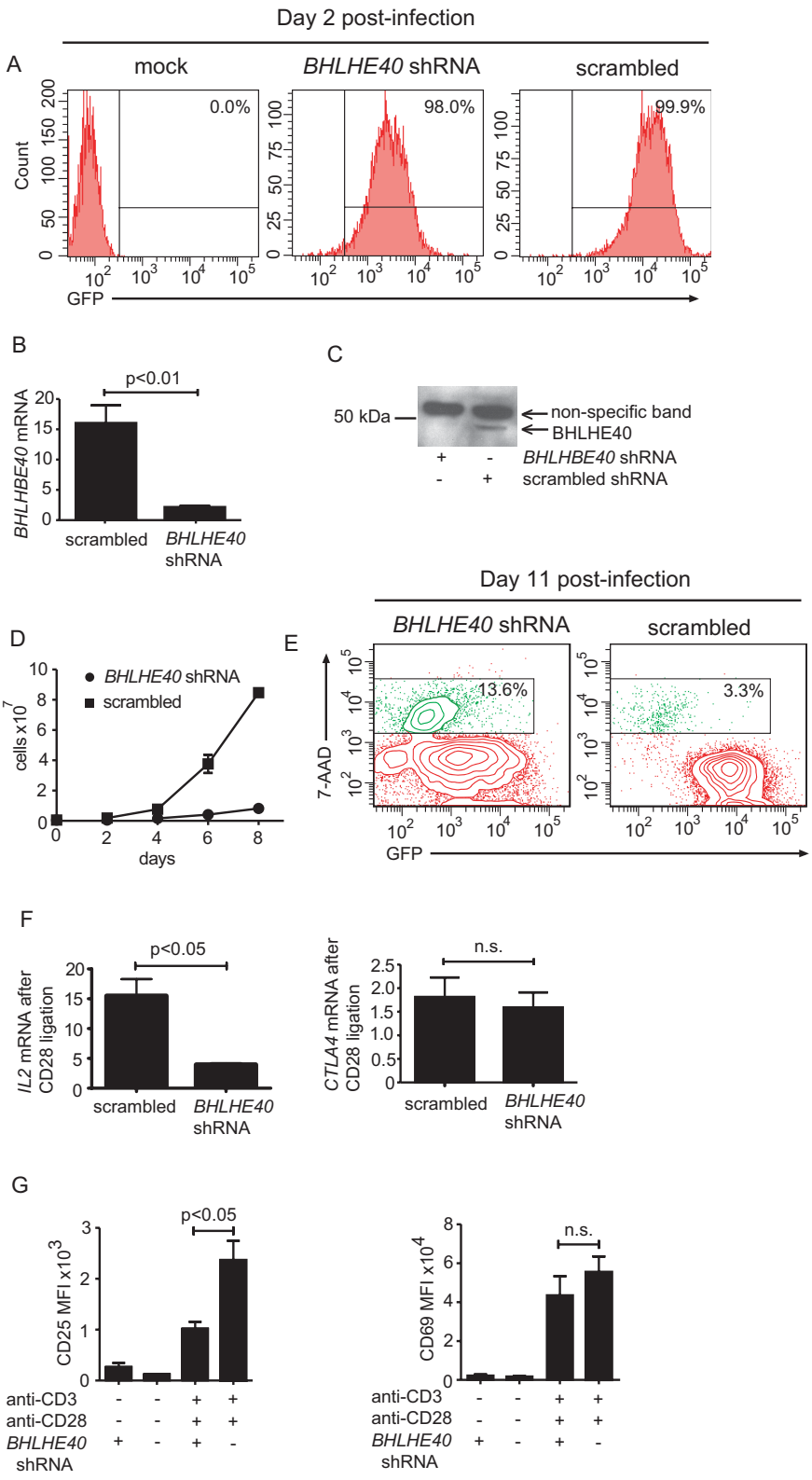

Figure 2.4. **Knock-down of BHLHE40 with an shRNA in Jurkat T cells blocks CD28 costimulation**. A, Jurkat T cells were infected with lentivirus containing pSICO-R vectors with an shRNA complementary to human BHLHE40 transcript or a scrambled shRNA. GPF expression at 48 hours indicated high transduction efficiency. B, RNA was harvested from Jurkat cells from part A and expression of BHLHE40 transcript was measured by

quantitative real-time PCR. BHLHE40 transcript is 7-fold decreased in resting Jurkat T cells transduced with a BHLHE40 shRNA-expressing lentivirus, compared to control. Results are from three independent experiments. Error bars are standard error of the mean. C, A Western blot analysis confirmed knock down of BHLHE40 protein in whole cell extracts from the Jurkat cells infected with shRNA-expressing virus. D, $1x10^6$ Jurkat cells previously infected with shRNA-expressing virus were seeded on day 0. Medium was added as necessary and live cells were counted every other day. The total number of cells in culture was followed for 8 days. Results are from three independent cultures. E, Jurkat T cells infected with a BHLHE40 shRNA-expressing lentivirus has more dead cells than the control cells (13.6% versus 3.3%), as marked by failure to exclude 7-AAD. The cells with the BHLHE40-specific shRNA also had more GFP^{lo} cells than control cells infected with a lentivirus expressing a scrambled shRNA. Results are representative of four independent experiments. F, Infected Jurkat cells were activated with anti-CD3 and anti-CD28 for 24 hours before harvesting RNA. IL-2 and CTLA-4 transcripts were measured by quantitative real time PCR. Expression in unstimulated cells is indexed to 1. G, Mean fluorescence intensity of CD25 is decreased in Jurkat T cells transduced with a BHLHE40 shRNA expressing lentivirus and then activated with anti-CD3 and anti-CD28 for 24 hours, compared to cells transduced with a scrambled control shRNA. CD69 upregulation was unaffected. Results are from 4 independent experiments. P values were determined by using unpaired T tests.

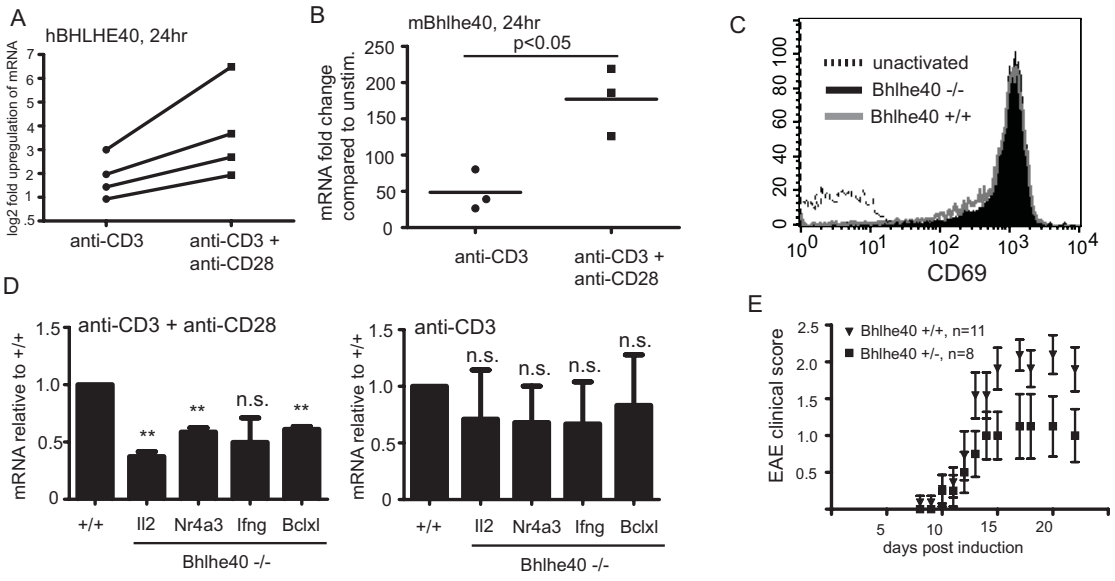

Figure 2.5. **Bhlhbe40 is necessary for maximal transcriptional response to CD28 costimulation.** A, BHLHE40 transcript was upregulated by CD28 costimulation in primary human CD4+CD45RA+ T cells. Lines connect data points from the same donor. B, Primary mouse CD4+CD62L+CD25- cells upregulate Bhlhe40 transcripts during CD28 costimulation. C, Primary mouse CD4+ T cells from *Bhlhe40* +/+ or -/- animals were activated *in vitro* for 24 hours. Cell surface expression of CD69 was similar between the two genotypes, indicating no defect in upregulation of this costimulation-independent activation marker. D, Expression of a panel of miRNA transcripts in primary mouse CD4+ T cells from *Bhlhe40* +/+ and -/- animals. Cells were activated with plate-bound antibodies, as indicated, for 24 hours before RNA harvest and real-time PCR analysis. E, Experimental autoimmune encephalitis was induced by using CFA and MOG 35-55 peptide.

BHLHE40	basic helix-loop-helix family, member e40
PPIF	peptidylprolyl isomerase F
SLC16A1	solute carrier family 16, member 1
FABP5	fatty acid binding protein 5
RBBP8	retinoblastoma binding protein 8
SOCS2	suppressor of cytokine signaling 2
BYSL	bystin-like
IRF8	interferon regulatory factor 8
CD83	CD83 molecule
F5	coagulation factor V (proaccelerin, labile factor)
LAMP3	lysosomal-associated membrane protein 3
TRAF1	TNF receptor-associated factor 1
LTA	lymphotoxin alpha (TNF superfamily, member 1)
TNF	tumor necrosis factor (TNF superfamily, member 2)
TNFRSF9	tumor necrosis factor receptor superfamily, member 9
MAP2K3	mitogen-activated protein kinase kinase 3
IL2	interleukin 2
TNFSF14	tumor necrosis factor (ligand) superfamily, member 14
SIK1	salt-inducible kinase 1
DUSP5	dual specificity phosphatase 5
CD200	CD200 molecule
IL2RA	interleukin 2 receptor, alpha
SPRY1	sprouty homolog 1, antagonist of FGF signaling
SLC43A3	solute carrier family 43, member 3
PGAP1	post-GPI attachment to proteins 1
TNFRSF4	tumor necrosis factor receptor superfamily, member 4
NAMPT	nicotinamide phosphoribosyltransferase
TBX21	T-box 21
C17orf96	chromosome 17 open reading frame 96
BIC	BIC transcript
PGAP1	post-GPI attachment to proteins 1
NAMPT	nicotinamide phosphoribosyltransferase

Table 2.1. **CD28 costimulation-induced genes.** This list includes the 32 transcripts with an increase in expression of more than 5-fold after anti-CD3 and anti-CD28 activation, compared to activation with anti-CD3 alone, at both 4 and 24 hours after activation.

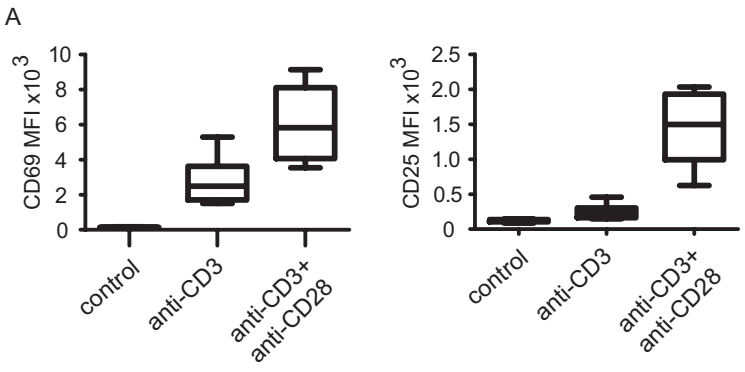

Supplemental Figure 2.1. **Expression of cell surface activation markers from all donors recruited for the microarray study**. PBMC was collected and CD4+CD45RA+ cells were sorted on a FACSAria. The cells were activated as described in Figure 1 and cell surface activation markers were analyzed by flow cytometry 24 hours late. The three donors with the highest CD69 MFI were used for subsequent microarray analysis. The box whiskers indicate the minimum and maximum values. The error bars are the standard error of the mean.

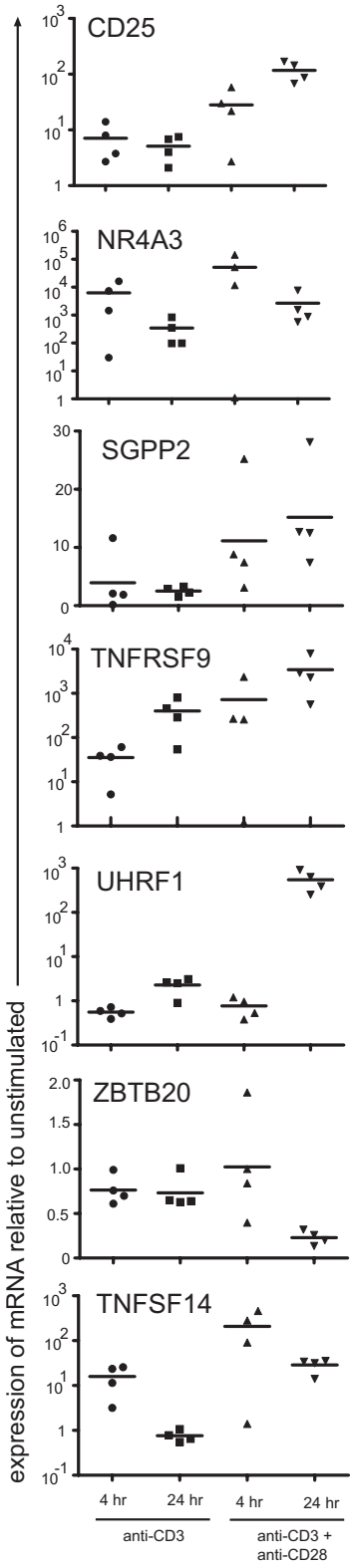

Supplemental Figure 2.2. **Microarray validation by quantitative real-time PCR**. A panel of 7 genes whose expression was highly differentially regulated by CD28 costimulation was chosen to validate the data from the microarray experiment. The same RNA samples used for the array were analyzed with Taqman real-time PCR primer-probe sets. A fourth donor not used in the microarray analysis was also included in this dataset. These data confirmed that the microarrays gave a good estimate of both the direction and relative magnitude of the changes in specific transcript levels after activation.

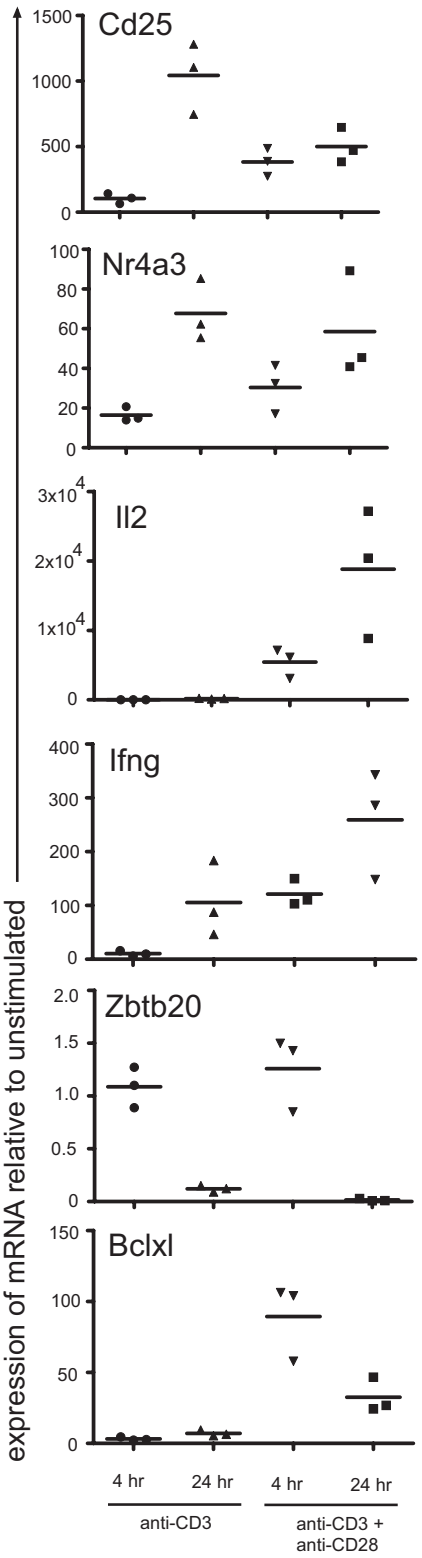

Supplemental Figure 2.3. **mRNA expression profiles of genes in activated mouse CD4+CD62L+CD25- T cells.** A panel of six genes whose expression was highly differentially regulated by CD28 costimulation in human CD4+ T cells was measured in naive mouse CD4+ T cells that were activated for 4 or 24 hours before harvest, as indicated. These data serve as a reference for the data presented in Figure 5D.

Supplemental table 1. Gene sets from GSEA.
Esensten et al.

4hr anti-CD3 vs 4hr anti-CD3+anti-CD28	**15 genes, max 100 permutations, q<0.1**						
Gene Set	Description	Total Genes	Genes found	p-value	q-value	ES	NES
CYTOPLASMIC_VESICLE_MEMBRANE	MIT Broad List c5	28	27	0	0.0596	0.75337	2.17347
CYTOPLASMIC_VESICLE_PART	MIT Broad List c5	28	27	0	0.0596	0.75337	2.17347
SECRETORY_GRANULE	MIT Broad List c5	18	18	0	0.0596	0.78761	2.06071
VESICLE_MEMBRANE	MIT Broad List c5	30	29	0	0.0596	0.72478	2.11982

24hr anti-CD3 vs. 4hr antiCD3+antiCD28	**15 genes, max 100 permutations, q<0.1**						
Gene Set	Description	Total Genes	Genes found	p-value	q-value	ES	NES
ORGANELLE_PART	MIT Broad List c5	1197	1161	0	0.0798	-0.5249	-1.81829
ORGANELLE_INNER_MEMBRANE	MIT Broad List c5	75	73	0	0.0866	-0.6922	-1.75879
CHROMATIN	MIT Broad List c5	35	35	0	0.0711	-0.6751	-1.92286
CYTOPLASMIC_PART	MIT Broad List c5	1385	1361	0	0.0757	-0.43	-1.87283
NUCLEAR_CHROMOSOME	MIT Broad List c5	54	54	0	0.0802	-0.5958	-1.82642
NUCLEAR_PART	MIT Broad List c5	579	549	0	0.09	-0.5673	-1.71922
CYTOPLASM	MIT Broad List c5	2137	2072	0	0.0746	-0.431	-1.89835
ORGANELLE_LUMEN	MIT Broad List c5	458	442	0	0.0961	-0.5582	-1.67859
ENDOPLASMIC_RETICULUM_MEMBRANE	MIT Broad List c5	85	84	0	0.0864	-0.498	-1.76373
ENDOPLASMIC_RETICULUM	MIT Broad List c5	294	288	0	0.0893	-0.4165	-1.72042
NUCLEAR_LUMEN	MIT Broad List c5	387	371	0	0.0962	-0.5326	-1.67478
NON_MEMBRANE_BOUND_ORGANELLE	MIT Broad List c5	632	618	0	0.0733	-0.4601	-1.97972
NUCLEUS	MIT Broad List c5	1433	1370	0	0.0945	-0.4626	-1.69056
ORGANELLE_MEMBRANE	MIT Broad List c5	299	293	0	0.0852	-0.5419	-1.7869
NUCLEAR_ENVELOPE_ENDOPLASMIC_RETICULUM_NETWOR	MIT Broad List c5	94	93	0	0.0896	-0.5019	-1.72787
ENVELOPE	MIT Broad List c5	169	163	0	0.0823	-0.6461	-1.80558
ENDOMEMBRANE_SYSTEM	MIT Broad List c5	220	215	0	0.0998	-0.4654	-1.65989
CONDENSED_NUCLEAR_CHROMOSOME	MIT Broad List c5	18	18	0	0.0858	-0.6634	-1.76612
ORGANELLE_ENVELOPE	MIT Broad List c5	169	163	0	0.0823	-0.6461	-1.80558
RUFFLE	MIT Broad List c5	32	30	0	0.0906	-0.573	-1.70897
RIBOSOME	MIT Broad List c5	39	39	0	0.0942	-0.62	-1.6879
NUCLEAR_ENVELOPE	MIT Broad List c5	73	70	0	0.0905	-0.5895	-1.71516
MEMBRANE_ENCLOSED_LUMEN	MIT Broad List c5	458	442	0	0.0961	-0.5582	-1.67859
INTRACELLULAR_NON_MEMBRANE_BOUND_ORGANELLE	MIT Broad List c5	632	618	0	0.0733	-0.4601	-1.97972
NUCLEAR_MEMBRANE	MIT Broad List c5	50	48	0	0.088	-0.6278	-1.74057

INTRACELLULAR_ORGANELLE_PART	MIT Broad List c5	1192	1156	0	0.0812	-0.5246	-1.81728
MACROMOLECULAR_COMPLEX	MIT Broad List c5	945	918	0	0.0707	-0.5155	-1.95244
MITOCHONDRION	MIT Broad List c5	343	335	0	0.0873	-0.6382	-1.76079
MITOCHONDRIAL_ENVELOPE	MIT Broad List c5	97	94	0	0.0963	-0.6869	-1.67164
CHROMOSOMAL_PART	MIT Broad List c5	96	96	0	0.0856	-0.626	-1.7954
NUCLEAR_MEMBRANE_PART	MIT Broad List c5	42	40	0	0.0962	-0.6755	-1.68174
PROTEIN_COMPLEX	MIT Broad List c5	816	803	0	0.0717	-0.4878	-1.96813
ENDOPLASMIC_RETICULUM_PART	MIT Broad List c5	97	96	0	0.0874	-0.5016	-1.74404
NUCLEOLUS	MIT Broad List c5	126	117	0	0.0845	-0.6641	-1.78523
SOLUBLE_FRACTION	MIT Broad List c5	161	159	0	0.0865	-0.4152	-1.75629
CHROMOSOME	MIT Broad List c5	124	123	0	0.0869	-0.592	-1.75926
NUCLEAR_CHROMOSOME_PART	MIT Broad List c5	34	34	0	0.0745	-0.6027	-1.98353
DNA_METABOLIC_PROCESS	MIT Broad List c5	257	255	0	0.0796	-0.5944	-1.82541
BIOPOLYMER_CATABOLIC_PROCESS	MIT Broad List c5	117	116	0	0.0802	-0.5348	-1.86431
RNA_METABOLIC_PROCESS	MIT Broad List c5	843	822	0	0.0819	-0.4218	-1.81497
DNA_REPAIR	MIT Broad List c5	125	123	0	0.0864	-0.605	-1.75029
MITOTIC_CELL_CYCLE_CHECKPOINT	MIT Broad List c5	21	21	0	0.084	-0.6843	-1.78101
NUCLEOBASE__NUCLEOSIDE_AND_NUCLEOTIDE_METABOLI	MIT Broad List c5	52	50	0	0.0803	-0.5838	-1.82903
ONE_CARBON_COMPOUND_METABOLIC_PROCESS	MIT Broad List c5	26	26	0	0.088	-0.494	-1.73251
CELL_DEVELOPMENT	MIT Broad List c5	579	574	0	0.0867	-0.3228	-1.75907
NEGATIVE_REGULATION_OF_APOPTOSIS	MIT Broad List c5	150	149	0	0.0698	-0.4404	-1.93817
BIOPOLYMER_METABOLIC_PROCESS	MIT Broad List c5	1687	1655	0	0.0793	-0.4008	-1.85868
MACROMOLECULAR_COMPLEX_ASSEMBLY	MIT Broad List c5	280	278	0	0.0891	-0.415	-1.72275
SECRETORY_PATHWAY	MIT Broad List c5	84	84	0	0.0963	-0.4055	-1.67724
MEIOSIS_I	MIT Broad List c5	20	20	0	0.0872	-0.6093	-1.75975
REGULATION_OF_DNA_REPLICATION	MIT Broad List c5	20	20	0	0.0966	-0.6602	-1.67042
NUCLEOBASE__NUCLEOSIDE__NUCLEOTIDE_AND_NUCLEIC	MIT Broad List c5	1246	1220	0	0.08	-0.4439	-1.83727
RESPONSE_TO_ENDOGENOUS_STIMULUS	MIT Broad List c5	200	196	0	0.0798	-0.5236	-1.85402
BIOSYNTHETIC_PROCESS	MIT Broad List c5	470	463	0	0.0726	-0.4275	-1.97626
M_PHASE	MIT Broad List c5	114	112	0	0.0905	-0.5364	-1.70772
PROGRAMMED_CELL_DEATH	MIT Broad List c5	434	431	0	0.0796	-0.3669	-1.83685
ORGANELLE_ORGANIZATION_AND_BIOGENESIS	MIT Broad List c5	474	462	0	0.0861	-0.4176	-1.76532
NUCLEAR_TRANSPORT	MIT Broad List c5	89	85	0	0.0963	-0.4678	-1.67375
REGULATION_OF_MITOSIS	MIT Broad List c5	41	40	0	0.0759	-0.5961	-1.87081
CARBOXYLIC_ACID_METABOLIC_PROCESS	MIT Broad List c5	178	174	0	0.0805	-0.4453	-1.84581
INTERPHASE	MIT Broad List c5	68	68	0	0.0875	-0.5253	-1.73622
AMINO_ACID_METABOLIC_PROCESS	MIT Broad List c5	78	76	0	0.0702	-0.5995	-1.93855

Supplemental Table 2.1. **Gene set enrichment analysis was performed to determine genes that were highly differentially regulated by CD28 costimulation.**

Chapter 3: The Tbx21 transcription factor in autoimmune diabetes

This chapter was originally published as "T-bet-Deficient NOD Mice Are Protected from Diabetes Due to Defects in Both T Cell and Innate Immune System Function." *Journal of Immunology*, 2009, 183: 75-82.

Abstract

The transcription factor T-bet (*Tbx21*) is critical for Th1 polarization of CD4+ T cells. Genetic deletion of *Tbx21* can cause either exacerbation or attenuation of different autoimmune diseases in animal models. In the non-obese diabetic (NOD) mouse, genetic deletion of the *Ifng* or the *Il12b* (IL12p40) genes, which are both critical Th1 cytokines, does not reduce the incidence of autoimmune diabetes. These results suggest that autoimmune diabetes in the NOD may not be a Th1-driven disease. However, we report that *Tbx21* deficiency in the NOD mouse completely blocks insulitis and diabetes due to defects both in the initiation of the anti-islet immune response and in the function of CD4+ effector T cells. We find defective priming of naive islet-reactive T cells by the innate immune system in $Tbx21^{-/-}$ animals. By contrast to naive cells, activated islet-reactive BDC2.5 TCR transgenic T cells do not require *Tbx21* in recipient animals for efficient adoptive transfer of diabetes. However, when these BDC2.5 TCR transgenic effector cells lack *Tbx21*, they are less effective at entering the pancreas and promoting diabetes than $Tbx21^{+/+}$ cells. $Tbx21^{-/-}$ regulatory T cells function normally *in vitro* and diabetes can be restored in $Tbx21^{-/-}$ mice by reducing Treg numbers. Thus, the absence of diabetes in the NOD.$Tbx21^{-/-}$ is due to intrinsic defects in both T cells and cells of the innate immune system paired with the relative preservation of regulatory T cell function.

Introduction

Germline deletion of the Th1-lineage transcription factor T-bet (*Tbx21*) can alternatively exacerbate or attenuate autoimmune and inflammatory diseases in animal models. *Tbx21* null animals have attenuated clinical symptoms of autoimmune experimental encephalomyelitis (1) and CD4+ *Tbx21* null cells do not cause colitis when transferred into SCID or Rag-deficient mice (2). *Tbx21* also plays a role in CD8+ T cell-driven disease. For example, ovalbumin-specific *Tbx21*-deficient CD8+ OT-I cells have intrinsic defects in tissue homing and cytotoxicity in a mouse model of myocarditis (3). Importantly, *Tbx21* null animals with a transgene expressing an LCMV protein in pancreatic islets are partially protected from diabetes when infected with LCMV due to defects in the generation of antiviral CD8+ T cells (4). In collagen antibody-induced arthritis in mice, *Tbx21* expression in dendritic cells was necessary to drive the disease in the absence of an adaptive immune response (5). *Tbx21*deficiency in B cells reduces autoantibody titers and renal immune complex deposition in Fas-deficient mice (6).

By contrast to these examples of attenuated disease, several disease models show exacerbated disease in the absence of *Tbx21*. *Tbx21*-deficient animals immunized with heart myosin develop exacerbated autoimmune myocarditis compared to controls due to increased IL-17 production by effector T cells (7). *Tbx21* null animals are more susceptible than wildtype animals to Th2-mediated diseases such as airway inflammation similar to human asthma (8) and bleomycin-induced skin sclerosis (9). Some strains of *Tbx21*-deficient mice that also lack an adaptive immune system due to *Rag2* gene deficiency develop spontaneous colitis due to dysregulated cytokine production in the gut mucosa (10). These examples show that *Tbx21* is important for the function of lymphocytes and non-lymphocytes in disease models and that the effects of *Tbx21* deficiency on a particular disease model are difficult to predict.

This complexity in different disease models is explained in part by the many different functions of *Tbx21* that have been described in lymphocytes and dendritic cells. CD8+ T cells

that lack *Tbx21* can produce IFN-gamma in vitro (11), likely due to the expression of the *Tbx21* paralogue Eomesodermin (12). However, the functions of *Tbx21* and Eomesodermin overlap only partially, since *Tbx21* null CD8+ T cells showed reduced IFN-gamma production in mice infected with *T. gondii* (13). *Tbx21* in dendritic cells promotes IFN-gamma production and is necessary for effective *in vivo* priming of antigen-specific T cells by DCs (14). Deficiency of *Tbx21* in B cells skews class switching away from IgG2a (6). Conversely, upregulation of *Tbx21* in cultured B cells is associated with decreased class switching to IgE and IgG1 (15). NK cells require *Tbx21* for control of tumor metastasis in mice inoculated with a melanoma cell line (16). NK cells that lack *Tbx21* have intrinsic cytotoxicity defects and survive poorly compared to $Tbx21^{+/+}$ NK cells in vivo and in vitro (16). In sum, *Tbx21* controls a wide range of Th1-related cellular phenotypes in many cell types of both the adaptive and the innate immune system.

There is evidence that polymorphisms in Th1-related genes contribute to risk of type 1 diabetes mellitus (T1DM)[5] in humans. A polymorphism of *Tbx21* that increases transcription from the IFN-gamma promoter has been implicated as a risk gene in human T1DM in a Japanese study population (17). However, the region of human chromosome 17 that contains *Tbx21* has not been implicated as a risk region for T1DM in a recent genome-wide association study (18). Separately, a polymorphism of the IL-12p40 gene has been linked to the risk of T1DM in humans (19).

Germline deletion of the *Ifng* gene or the IFN-gamma receptor gene has been reported to delay only slightly the onset of diabetes in the NOD mouse (20-23). Since *Tbx21* drives IFN-gamma production in both CD4+ T cells (11) and dendritic cells (14), we sought to test whether *Tbx21* was required for spontaneous autoimmune diabetes by backcrossing the *Tbx21* null mouse to the NOD. Our results show that loss of *Tbx21* completely blocks diabetes in NOD mice. The

[5] Abbreviations used in this paper: NOD, non-obese diabetic; T1DM, Type 1 diabetes mellitus; Treg, regulatory T cell; SNP, single nucleotide polymorphism.

NOD.*Tbx21*$^{-/-}$ mice are protected from insulitis and show defects in both effector T cell function and in innate immune cell function. Regulatory T cells (Tregs) in NOD.*Tbx21*$^{-/-}$ animals function normally in *in vitro* and *in vivo* assays, suggesting that the balance of effector versus regulatory function of T cells is tipped toward regulation in these animals. Our results suggest that spontaneous diabetes in the NOD mouse requires a *Tbx21*-dependent Th1 response and that *Tbx21* impacts disease pathogenesis in multiple cell types. A role for the Th1 T cell subset in diabetes in the NOD mouse was previously uncertain (22). Thus, our results highlight the importance of the Th1 effector function for diabetes in the NOD mouse.

Materials and Methods

Mice

Mice with the *Tbx21*^{tm1Glm} allele were backcrossed to NOD/MrkTac mice purchased from Taconic Farms. NOD.BDC2.5 TCR-transgenic, NOD.Cg-Rag2^{tm1Fwa}/JbsJ, and NOD.129S2(B6)-Cd28^{tm1Mak}/JbsJ mice were bred and housed in a specific pathogen-free barrier facility at the University of California, San Francisco. A scan of SNPs across the genome of the NOD.*Tbx21*$^{-/-}$ mouse revealed that all chromosomes were NOD-derived except for the telomeric end of chromosome 11, which contains *Tbx21* (Supplemental Table 1[6]). Diabetes incidence was followed by periodic checks for elevated urine glucose levels using Diastix strips (Bayer Corp., Elkhart IN) and confirmed with blood glucose measurements of >250 mg/dL on at least two separate days using an Accu-Chek glucose meter (Roche). All animal experiments were approved by the University of California, San Francisco, Animal Care and Use Committee.

Histopathology

Pancreata were harvested and immediately fixed in 10% buffered formalin, embedded in paraffin, sectioned, and stained with H&E. Scoring of insulitis was done blinded to the genotype of the mouse, according to the protocol found in (24).

Cell culture and adoptive transfer

For activation assays, CD4+ T cells from NOD and NOD.*Tbx21*$^{-/-}$ and $^{+/-}$ mice were purified from bulk lymph node cells with a RoboSep (StemCell Technologies, Vancouver BC) and the StemCell mouse CD4+ T cell enrichment kit or with an AutoMACS (Miltenyi Bitech, Auburn CA). Cell purities were typically >90% CD4+. For adoptive transfer experiments, CD4+CD25^{+} cells were removed by incubating cells for 20 minutes in supernatant from the anti-CD25 hybridoma 7D4 (IgM) followed by incubation with rabbit complement for 30 minutes at 37^{o}C. For in vitro activation experiments, cells were resuspended in DMEM supplemented with

[6] The published version of this article contains additional supplemental material.

10% FBS, glutamine, HEPES buffer, beta-mercaptoethanol (0.1%), non-essential amino acids, and antibiotics. The cells were activated in plates pre-coated with 1 ug/mL anti-CD3 (clone 145-2C11) and 1 ug/mL anti-CD28 (clone PV1). For Th1 skewing, the medium was supplemented with 100 U/mL recombinant human IL-2 (Proleukin, Prometheus Laboratories, San Diego, CA), 20 ng/mL recombinant mouse IL-12 (Peprotech, Rocky Hill NJ), and 20 ug/mL anti-IL-4 (clone 11B.11). For adoptive transfer experiments with naive T cells, CD4+ cells were isolated as described above and injected into recipient mice via the tail vein. For adoptive transfer experiments with activated BDC2.5 transgenic cells, the cells were isolated as described above and activated by mixing together the mimotope peptide p31 (25) with T-depleted, irradiated splenocytes from non-diabetic NOD mice. Activation was done in supplemented DMEM as described above without skewing cytokines. Cells were collected 4 days after activation and adoptively transferred into mice via tail vein injection.

RNA isolation and real-time PCR

RNA from primary mouse T cells was extracted using the RNAeasy kit (Qiagen, Valencia CA) using the manufacturer's recommended protocol. Reverse transcription was done with a SuperScriptIII reverse transcriptase kit (Invitrogen, Carlsbad CA) using random DNA hexamers as primers, according to the manufacturer's instructions. Real-time PCR was performed on a 7500 Fast Real-time PCR System (Applied Biosystems, Foster City CA) using Taqman primer probes Mm99999054_s1 (*Cxcr3*) and Mm00801778_m1 (*Ifng*) with a Taqman primer-probe set for the eukaryotic 18S rRNA as an internal control. cDNA was diluted 10,000-fold for assay of 18S rRNA levels. Both the *Cxcr3* and *Ifng* primer-probes were validated before use by titration against the 18S rRNA primer-probe using lymphocyte cDNA and the amplification efficiency of the individual primer-probes was calculated. Calculation of relative expression was done using the ΔΔCt method, according to the recommendations from Applied Biosystems.

Flow cytometry

Intracellular staining for FOXP3 was carried out with the eBioscience FOXP3 staining kit, according to the manufacturer's instructions. For CXCR3 surface standing, spleens were harvested, disrupted, and the splenocytes were incubated for 10 minutes in supernatant from the anti-CD16+CD32 hybridoma 2.4G2 to block non-specific binding of IgG to splenocytes. Primary stain was done for 30 minutes with purified goat anti-mouse CXCR3, SC-9902 (Santa Cruz Biotechnology, Santa Cruz CA) at 1:5 dilution. As a control stain, this primary Ab was omitted. Cells were washed and incubated with $F(ab')^2$ biotin-conjugated donkey anti-goat (Jackson Immunoresearch, West Grove PA) for 30 minutes. Cells were washed again and PE-conjugated streptavidin (BD Biosciences, San Jose CA) was added for 30 minutes. BDC TCR surface staining was done with anti-BDC clonotype mAb (26). The secondary Ab was biotin-conjugated rat anti-mouse IgG2b (BD Biotechnologies, San Jose, CA), which was detected with PE-conjugated streptavidin (BD Biotechnologies, San Jose, CA). Cells were washed between all incubation steps. All cytometry data were collected on a BD Biosciences FACSCalibur or LSRII machine.

CFSE labeling

CD4+CD25$^-$ T cells were resuspended at 20×10^6 cells/mL in PBS. CFSE at a stock concentration of 10 mM (Invitrogen/Molecular Probes, Carlsbad CA) was diluted 1:2,000 in PBS and this dilution was mixed with an equal volume of cells. After 5 minutes, the reaction was quenched with FBS and the cells were collected for adoptive transfer.

Treg isolation and expansion

Treg cells were sorted from polyclonal lymph node cells isolated from NOD and NOD.*Tbx21*$^{-/-}$ animals. Suppression assays in 96-well plates were set up as previously described (27). BDC2.5 TCR transgenic Tregs were FACS purified and expanded *in vitro* as previously described before adoptive transfer of 3×10^6 cells into *NOD.Cd28-/-* mice (27).

Mouse genome SNP scan

A scan of SNPs (single nucleotide polymorphisms) across the genome of the NOD.*Tbx21*$^{-/-}$ mice was done by the UT Southwestern Medical Center Microarray Core Facility using a Mouse Medium Density Linkage Panel (Illumina, San Diego, CA).

Results

Tbx21$^{-/-}$ mice are protected from diabetes

The *Tbx21*$^{-/-}$ mouse was backcrossed to NOD for 10 generations. A scan of SNPs throughout the genome of the NOD.*Tbx21*$^{-/-}$ mouse revealed that all chromosomes were NOD-derived except for part of chromosome 11, which contains the null allele of *Tbx21* (Supplemental Table 3.1). To determine diabetes incidence in these animals, female offspring of NOD.*Tbx21*$^{+/-}$ parents were followed for diabetes incidence for 30 weeks. Both NOD.*Tbx21*$^{-/-}$ and NOD.*Tbx21*$^{+/-}$ animals were completely protected from disease (Figure 3.1A). The NOD.*Tbx21*$^{+/+}$ littermates became diabetic with normal kinetics for our colony, with 56% of female mice diabetic by 30 weeks of age. Histological analysis of pancreata showed that 12-week old NOD.*Tbx21*$^{-/-}$ females are protected from insulitis (Figure 3.1B). Heterozygous mice show partial protection from insulitis, indicating that gene dosage of *Tbx21* affects progression to insulitis.

Priming of diabetogenic T cells is defective in *Tbx21*$^{-/-}$ mice

Since defects in APC function have been described in *Tbx21*$^{-/-}$ mice (14), we tested initial priming of diabetogenic T cells in *Tbx21*$^{-/-}$ hosts. Naive CD4+CD25^{-} BDC2.5 TCR transgenic cells, which have a TCR specific for an islet antigen in the context of I-A^{g7} (28), were labeled with CFSE and adoptively transferred into NOD or NOD.*Tbx21*$^{-/-}$ recipients. After three days, the pancreatic lymph nodes of the recipient mice were harvested and analyzed by flow cytometry. The percentage of *Tbx21*$^{+/+}$ BDC2.5 TCR transgenic T cells that went into cycle in the pancreatic lymph nodes of the recipient animals was reduced by about half in the *Tbx21*$^{-/-}$ recipients (Figure 3.2A). Deficiency of *Tbx21* in the T cells did not affect proliferation when the recipients were NOD.*Tbx21*$^{+/+}$. Interestingly, *Tbx21* deficient cells proliferated better in NOD.*Tbx21*$^{-/-}$ hosts compared to NOD.*Tbx21*$^{+/+}$ cells in NOD.*Tbx21*$^{-/-}$ hosts ($p<0.01$), suggesting that NOD.*Tbx21*$^{+/+}$ T cells may have a greater requirement for *Tbx21* in antigen-presenting cells than NOD.*Tbx21*$^{-/-}$ T

cells. In sum, the expression of *Tbx21* in the recipient animals was critical for optimal priming of diabetogenic T cells.

To test for a functional role of *Tbx21* in APCs that prime autoreactive diabetogenic T cells, low numbers of naive CD4+CD25^{-}*Tbx21*$^{+/+}$ BDC2.5 TCR transgenic cells were transferred into *Rag2*$^{-/-}$ animals. At a dose of 5×10^3 BDC2.5 transgenic cells per mouse, all of the *Tbx21*$^{+/+}$ recipients, but only 3 of 12 *Tbx21*$^{-/-}$ recipients had become diabetic by 90 days after adoptive transfer. At a high dose of 1×10^6 cells per animal, all recipients became diabetic between 11 and 21 days after adoptive transfer, regardless of the *Tbx21* genotype of the recipient animal (Figure 3.2B). These results suggest that there is a defect in T cell priming in *Tbx21*$^{-/-}$ mice after adoptive transfer of a low number of autoreactive T cells. However, this defect can be overcome with the transfer of higher cell numbers. A statistically significant difference (p=0.03) was found between the percentage of CD4+ cells in the pancreatic lymph nodes of *Tbx21*$^{+/+}$ and *Tbx21*$^{-/-}$ recipient mice 11 days after adoptive transfer. In the *Tbx21*$^{+/+}$ recipients, 20% (range 14.8% to 23%, n=3) of cells were CD4+, compared to 11.1% (range 10.5% to 12.1%, n=3) of cells in the *Tbx21*$^{-/-}$ recipients. Together, these results suggest that *Tbx21* is necessary in the innate immune system for efficient priming and proliferation of diabetogenic T cells.

Effector T cells require *Tbx21* for efficient disease transfer

Different numbers of naive CD4+CD25^{-} *Tbx21*$^{-/-}$ BDC2.5 transgenic T cells were transferred into *Rag2*$^{-/-}$ recipients to test for the capacity of the *Tbx21*-deficient cells to cause diabetes. When 1×10^6 *Tbx21*$^{-/-}$ cells were transferred, all *Rag2*$^{-/-}$.*Tbx21*$^{+/+}$ and *Rag2*$^{-/-}$.*Tbx21*$^{-/-}$ animals became diabetic with rapid kinetics (Figure 3.2C). However, when only 5×10^3 cells were transferred, the disease incidence was decreased to 8% (*Tbx21*$^{-/-}$ cells into *Rag2*$^{-/-}$.*Tbx21*$^{+/+}$ hosts, n=12) and 20% (*Tbx21*$^{-/-}$ cells into *Rag2*$^{-/-}$.*Tbx21*$^{-/-}$ hosts, n=11), by 50 days after adoptive transfer. By comparison, when 5×10^3 naive CD4+CD25^{-} *Tbx21*$^{+/+}$ BDC2.5 transgenic T cells were transferred into Rag$^{-/-}$.*Tbx21*$^{+/+}$ animals, 100% of mice became diabetic within 40 days of

adoptive transfer (Figure 3.2B). These results show a clear defect in the ability of *Tbx21*-deficient T cells to cause diabetes when the number of diabetogenic cells is limited in this system.

In the experiments described above, differences in initial priming and homeostatic expansion could account for the observed defects in *Tbx21*-deficient T cells. We sought to test for a cell-intrinsic defect in the *Tbx21*$^{-/-}$ T cells unrelated to these processes. Lymph nodes were harvested from BDC2.5 TCR transgenic NOD or NOD.*Tbx21*$^{-/-}$ mice and CD4+ cells were purified by magnetic bead selection. These cells were then cultured with T cell-depleted irradiated splenocytes from NOD mice in the presence of the peptide mimetope Acp31. After four days, no difference in T cell proliferation (Figure 3.3A) or CD25 expression (data not shown) were detected between the *Tbx21*$^{-/-}$ and $^{+/+}$ transgenic cells.

Adoptive transfer of 1×10^6 of these activated cells into NOD or NOD.*Tbx21*$^{-/-}$ animals revealed that activated *Tbx21*$^{-/-}$ T cells induce diabetes at lower rates and with slower kinetics than activated *Tbx21*$^{+/+}$ cells (Figure 3.3B). These results show that *Tbx21* is required in the activated transgenic T cells but not in the recipient animals for robust diabetes transfer. These results could be explained by a defect in tissue trafficking in the activated *Tbx21*$^{-/-}$ cells or by some other intrinsic defect in effector function. To distinguish between these possibilities, we harvested pancreata from pre-diabetic animals from the above experiment at day 5 post-transfer for histological scoring of islet infiltration. This analysis showed that the animals transferred with activated *Tbx21*$^{-/-}$ T cells had infiltration in fewer than 50% of their islets (Figure 3.3C). By contrast, animals transferred with activated *Tbx21*$^{+/+}$ BDC2.5 T cells showed complete destruction of more than 75% of their islets, with few islets free of mononuclear infiltration.

In a study of autoimmune myocarditis induced by activated *Tbx21*$^{-/-}$ transgenic T cells, it was found that these cells become sequestered in the heart draining lymph node after adoptive transfer, likely due to a defect in CXCR3 expression (3). However, TCR-specific staining of activated BDC2.5 TCR$^+$ T cells revealed no significant differences in the percentage of transgenic

T cells among the total CD4+ population of the pancreatic lymph nodes of recipients of activated BDC2.5 T cells 5 days after adoptive transfer (Figure 3.4A). To test if differences in CXCR3 expression could play a role in the efficacy of BDC2.5 T cell transfers, *Cxcr3* mRNA was measured by quantitative PCR in the activated BDC2.5 TCR^+ T cells used for the adoptive transfer experiments described above. *Ifng* expression was decreased 100-fold in *Tbx21*-deficient T cells. In contrast, *Cxcr3* mRNA expression in $Tbx21^{-/-}$ T cells was decreased to 25% of the levels in $Tbx21^{+/+}$ T cells (Figure 3.4B). Thus, the activated $Tbx21^{-/-}$ T cells appeared to enter the pancreas in lower numbers than $Tbx21^{+/+}$ T cells although they were not sequestered in the pancreatic lymph nodes despite lower amounts of CXCR3 expression. $Tbx21^{+/-}$ CD4+ T cells activated under Th1 skewing conditions showed an intermediate phenotype, with *Ifng* mRNA and protein expression decreased by half and *Cxcr3* mRNA expression levels between 80 and 96% of $Tbx21^{+/+}$ (Supplemental Figure 3.1A and B). These results are consistent with previous reports showing that a single copy of *Tbx21* is not sufficient to drive normal immune cell effector function (8, 29). The decrease in *Cxcr3* expression in $Tbx21^{-/-}$ cells in the experiments described above was modest as compared to the observed 30-fold decrease in *Cxcr3* mRNA previously reported in CD4+ cells activated in a Th0 culture (30) and even larger decreases reported in other settings (3). In fact, surface staining revealed only a modestly lower level of CXCR3 protein expression on freshly isolated $Tbx21^{-/-}$ CD4+ splenocytes as compared to $Tbx21^{+/+}$ controls (Figure 3.4C). Although this difference was statistically significant in splenic CD4+ T cells, there was no difference in CXCR3 protein expression between $Tbx21^{+/+}$ and $^{-/-}$ splenic CD8+ T cells (Figure 3.4D).

Regulatory T cells contribute to protection of *Tbx21*-deficient mice from diabetes

CD4+FOXP3+ Treg function is critical for controlling the balance between effector function and regulation in diabetes in the NOD mouse (31). There was no difference in the percentage of FOXP3+ cells among total CD4+ T cell populations in the spleen or pancreatic

lymph nodes of 6-week old pre-diabetic NOD and *NOD.Tbx21-/-* mice (Figure 3.5A). As shown in Figure 3.5B, *Tbx21-/-* Tregs were able to suppress *Tbx21+/+* effector cell proliferation with the same efficiency as *Tbx21+/+* Tregs. Given the defects in effector function described above, we sought to test whether the dominant regulatory role of FOXP3+ cells was responsible for preventing diabetes in the *NOD.Tbx21-/-* animal. To test this hypothesis, the NOD.Tbx21-/- mice were crossed onto a *NOD.CdD28-/-* background. The *NOD.Cd28-/-* mouse exhibits rapid, synchronized diabetes onset at about 12 weeks of age due to a defect in Treg survival and function (31). In contrast to the *NOD.Tbx21-/-* mice, the *NOD.Tbx21-/-.Cd28-/-* animals showed diabetes onset starting from 9 weeks of age. Overall incidence of diabetes in this genotype increased until about 20 weeks of age before reaching a plateau at 72% (Figure 3.6A). These data suggest that *Tbx21-/-* Tregs are necessary *in vivo* to prevent diabetes. To more rigorously test this hypothesis, *NOD.Cd28-/-* mice were adoptively transferred with *in vitro* expanded *NOD.BDC2.5* Tregs that were either *Tbx21-/- or +/+*. The recipient mice were then followed for spontaneous diabetes incidence (Figure 3.6B). Protection of *Cd28-/-* mice from diabetes with *Tbx21-/-* Tregs was statistically significant (log rank test, $p<0.05$). There was no statistical difference between the groups treated with *Tbx21+/+* and *Tbx21-/-* Tregs (log rank test, $p=0.16$). Lastly, we bred *NOD.Tbx21-/-* mice that expressed the BDC2.5 transgene and were also Rag2-deficient. These animals showed rapid diabetes onset at or soon after weaning (Figure 3.6C), similar to published data on this genotype in the context of Tbx21 sufficiency (32). By contrast, *Rag2+/+* animals were protected from early onset of diabetes (log rank test, $p<0.01$). These results point to a critical role for regulatory T cells in controlling diabetes in Tbx21-deficient animals, because expression of endogenously rearranged TCRα chains is necessary for the generation of BDC2.5 Tregs.

Discussion

In this paper, we show that the Tbx21 transcription factor, which is a critical regulator of Th1 responses, is necessary for diabetes in the NOD mouse. We have found defects in both the innate and adaptive immune systems in the NOD.*Tbx21*$^{-/-}$ mouse. Cells of the innate immune system in *Tbx21*$^{-/-}$ mice are defective in driving activation and cycling of adoptively transferred naive BDC2.5 TCR transgenic T cells. This cycling defect was paralleled by a defect in diabetes transfer by naive islet-reactive cells into *Rag2*$^{-/-}$.*Tbx21*$^{-/-}$ mice. The observed failure of small numbers of anti-islet Ag-specific transgenic T cells to cause disease could be overcome with high numbers of cells. This result suggests that efficient *in vivo* proliferation, which is absent in *Tbx21*$^{-/-}$ recipients, is critical to generate large enough numbers of islet-reactive cells to cause disease. The defects in initial T cell priming and proliferation helps to explain why the NOD.*Tbx21*$^{-/-}$ animals fail to develop insulitis, which is normally completely penetrant in the NOD mouse (34). Further work with a conditional allele of *Tbx21* will more clearly elucidate the role of this transcription factor in cells of the innate immune system.

In addition to defects in the innate immune system, there are also profound defects in diabetogenic CD4+ T cells that lack *Tbx21*. Activated NOD.BDC2.5 TCR transgenic T cells that lack *Tbx21* fail to enter the pancreas and cause islet destruction similar to *Tbx21*$^{+/+}$ cells. The *Tbx21*$^{-/-}$ cells were not sequestered in the target organ draining lymph nodes, a result reported in another adoptive transfer model using transgenic *Tbx21*$^{-/-}$ cells (3). Expression of *Cxcr3* mRNA is decreased in *Tbx21*$^{-/-}$ BDC2.5 TCR transgenic T cells activated in vitro compared to *Tbx21*$^{+/+}$ cells. However, this decrease is much more modest (25% of WT) than that described by others in *Tbx21*$^{-/-}$ cells (3, 30). By contrast, IFN-γ expression is completely dependent upon *Tbx21* expression. This modest difference in CXCR3 expression implies that the trafficking defects in *Tbx21*$^{-/-}$ T cells may be due to other factors besides decreased CXCR3 expression. We speculate that *Tbx21* is important in the innate immune system in the early initiating stages of autoimmune

diabetes and that the T cell defects become relevant at later stages of pathogenesis after the generation of activated effector T cells.

The absence of diabetes in the NOD.*Tbx21*$^{-/-}$ mouse is unexpected. Although there is some evidence that Th1 cytokines such as IL-12 help to promote diabetes in the NOD (35, 36), both the IL-12-deficient (37) and the IFN-γ deficient (20) NOD mice show robust progression to diabetes. These results have led to uncertainty about the importance of IFN-γ-producing Th1 T cells in the pathogenesis of diabetes in the NOD. Importantly, a recent report argues that IFN-γ can protect against diabetes by decreasing a pathogenic anti-islet Th17 response (38). These results raise the prospect that diabetes in the NOD is a Th17-driven disease. This hypothesis is unlikely for two reasons. First, *Stat4*$^{-/-}$ mice on the NOD background are mostly, but not completely protected from diabetes (39, 40). Stat4 is critical for IL-12 receptor signaling (41) and its functions in driving gene expression during Th1 differentiation only partially overlap with those of *Tbx21* (42). Second, we have found that the phenotype of the NOD.*Tbx21*$^{-/-}$ mouse is even stronger than the *NOD.Stat4*$^{-/-}$ because none of the *Tbx21*$^{-/-}$ NOD mice develop diabetes or exhibit insulitis. This profound block in diabetes and insulitis shows that the effects of Tbx21 in diabetes extended beyond driving IFN-γ production. Indeed, many other reports have shown that *Tbx21* is necessary not only for the production of IFN-γ or IL-12, but also for a wide range of phenotypes including lymphocyte trafficking (30), cytotoxic activity of T cells (43), and priming of T cells by dendritic cells (14).

The 129S6/SvEvTac-derived genetic region surrounding the Tbx21 null allele in the NOD.*Tbx21*$^{-/-}$ mouse extends for up to 15 Mb, raising the possibility that 129-derived genes other than *Tbx21* could contribute to the protection of the NOD.*Tbx21*$^{-/-}$ mouse from diabetes. Importantly, chromosome 11 contains *Idd4* (44-46), a region initially derived from B10.H-2^{g7} mice that partially protects NOD mice from developing diabetes. In these studies, mice heterozygous for the C57BL/10-derived portion of chromosome 11 had rates of diabetes of about

half of the homozygous controls and similar amounts of insulitis (45). Several other non-NOD regions spread along the length of mouse chromosome 11 have been associated with protection from diabetes, but none of the NOD.Idd4 congenic mice in the literature show a complete absence of diabetes as observed in the *Tbx21*$^{+/-}$ and *Tbx21*$^{-/-}$ mice (47-49). The region of chromosome 11 defined as Idd4 by the Jackson Laboratory is completely NOD-derived in the NOD.*Tbx21*$^{-/-}$ mouse (Supplemental Table 3.1). Thus, although we cannot exclude the possibility that some part of the observed phenotype of the NOD.*Tbx21*$^{-/-}$ mouse is due to 129-derived genes linked to *Tbx21*, the genetic ablation of *Tbx21* is very likely to be critical for a large part of the observed phenotype of the mouse.

Regulatory T cells play a role in controlling diabetes in the NOD.*Tbx21*$^{-/-}$ mouse. Deficiency of CD28 in the NOD mouse has been shown to decrease the number of Tregs and increase the kinetics and penetrance of diabetes (50). Strikingly, the NOD.*Tbx21*$^{-/-}$.CD28$^{-/-}$ mouse shows robust progression to diabetes, implying that *Tbx21*$^{-/-}$ Tregs are necessary to prevent disease in this animal. To directly test whether *Tbx21*$^{-/-}$ Tregs are capable of preventing diabetes *in vivo*, we adoptively transferred *in vitro* expanded BDC2.5 Tregs that were either *Tbx21*$^{+/+}$ or $^{-/-}$ into *NOD.Cd28-/-* mice. The *Tbx21*$^{-/-}$ Tregs are competent to prevent or delay disease in these animals compared to untreated controls. However, 2 of 5 *Cd28*$^{-/-}$ mice in the group treated with *Tbx21*$^{-/-}$ Tregs became diabetic during the course of the experiment, compared to 0 of 5 in the *Tbx21*$^{+/+}$ Treg-treated group. These results suggest that although *Tbx21*$^{-/-}$ Tregs are functional, they may be less effective than *Tbx21*$^{+/+}$ Tregs at similar doses. However, the survival curve of the mice treated with *Tbx21*$^{-/-}$ Tregs was not statistically different from those treated with *Tbx21*$^{+/+}$ Tregs. Further, NOD.*Rag2*$^{-/-}$.*Tbx21*$^{-/-}$.BDC2.5 TCR transgenic mice, which lack endogenous regulatory T cells, show rapid progression to diabetes between 4 and 8 weeks of age. Taken together, these data demonstrate that regulatory T cells contribute to the control of diabetes in *Tbx21*$^{-/-}$ animals and that *Tbx21*$^{-/-}$ effector cells are still competent to cause diabetes if

regulatory T cells are removed. Thus, the balance between regulation and autoimmunity in the NOD is shifted toward tolerance by the deficiency in *Tbx21*, but the system can still be pushed into autoimmunity. Additional studies using tissue-specific genetic deletion of *Tbx21* will be needed to define precisely which *Tbx21*-expressing cell types are the most important for spontaneous diabetes in the NOD.

Acknowledgements

We thank members of the Bluestone laboratory for helpful advice. We thank X. Zhang and the UCSF Helen Diller Family Comprehensive Cancer Center Mouse Pathology Core for assistance with preparation of H&E slides. We thank Paul Wegfahrt and Nicolas Martinier for assistance with mouse handling and Shuwei Jiang for assistance with sorting Tregs. We thank Dimitri de Kouchkovsky for assistance with genotyping mice.

References

1. Bettelli, E., B. Sullivan, S. J. Szabo, R. A. Sobel, L. H. Glimcher, and V. K. Kuchroo. 2004. Loss of T-bet, but not STAT1, prevents the development of experimental autoimmune encephalomyelitis. *J Exp Med 200:79-87*.

2. Neurath, M. F., B. Weigmann, S. Finotto, J. Glickman, E. Nieuwenhuis, H. Iijima, A. Mizoguchi, E. Mizoguchi, J. Mudter, P. R. Galle, A. Bhan, F. Autschbach, B. M. Sullivan, S. J. Szabo, L. H. Glimcher, and R. S. Blumberg. 2002. The transcription factor T-bet regulates mucosal T cell activation in experimental colitis and Crohn's disease. *J Exp Med 195:1129-1143*.

3. Taqueti, V. R., N. Grabie, R. Colvin, H. Pang, P. Jarolim, A. D. Luster, L. H. Glimcher, and A. H. Lichtman. 2006. T-bet controls pathogenicity of CTLs in the heart by separable effects on migration and effector activity. *J Immunol 177:5890-5901*.

4. Juedes, A. E., E. Rodrigo, L. Togher, L. H. Glimcher, and M. G. von Herrath. 2004. T-bet controls autoaggressive CD8 lymphocyte responses in type 1 diabetes. *J Exp Med 199:1153-1162*.

5. Wang, J., J. W. Fathman, G. Lugo-Villarino, L. Scimone, U. von Andrian, D. M. Dorfman, and L. H. Glimcher. 2006. Transcription factor T-bet regulates inflammatory arthritis through its function in dendritic cells. *J Clin Invest 116:414-421*.

6. Peng, S. L., S. J. Szabo, and L. H. Glimcher. 2002. T-bet regulates IgG class switching and pathogenic autoantibody production. *Proc Natl Acad Sci U S A 99:5545-5550*.

7. Rangachari, M., N. Mauermann, R. R. Marty, S. Dirnhofer, M. O. Kurrer, V. Komnenovic, J. M. Penninger, and U. Eriksson. 2006. T-bet negatively regulates autoimmune myocarditis by suppressing local production of interleukin 17. *J Exp Med 203:2009-2019*.

8. Finotto, S., M. F. Neurath, J. N. Glickman, S. Qin, H. A. Lehr, F. H. Green, K. Ackerman, K. Haley, P. R. Galle, S. J. Szabo, J. M. Drazen, G. T. De Sanctis, and L. H. Glimcher. 2002. Development of spontaneous airway changes consistent with human asthma in mice lacking T-bet. *Science 295:336-338*.

9. Aliprantis, A. O., J. Wang, J. W. Fathman, R. Lemaire, D. M. Dorfman, R. Lafyatis, and L. H. Glimcher. 2007. Transcription factor T-bet regulates skin sclerosis through its function in innate immunity and via IL-13. *Proc Natl Acad Sci U S A 104:2827-2830*.

10. Garrett, W. S., G. M. Lord, S. Punit, G. Lugo-Villarino, S. K. Mazmanian, S. Ito, J. N. Glickman, and L. H. Glimcher. 2007. Communicable ulcerative colitis induced by T-bet deficiency in the innate immune system. *Cell 131:33-45*.

11. Szabo, S. J., B. M. Sullivan, C. Stemmann, A. R. Satoskar, B. P. Sleckman, and L. H. Glimcher. 2002. Distinct effects of T-bet in TH1 lineage commitment and IFN-gamma production in CD4 and CD8 T cells. *Science 295:338-342*.

12. Pearce, E. L., A. C. Mullen, G. A. Martins, C. M. Krawczyk, A. S. Hutchins, V. P. Zediak, M. Banica, C. B. DiCioccio, D. A. Gross, C. A. Mao, H. Shen, N. Cereb, S. Y. Yang, T. Lindsten, J. Rossant, C. A. Hunter, and S. L. Reiner. 2003. Control of effector CD8+ T cell function by the transcription factor Eomesodermin. *Science 302:1041-1043*.

13. Mayer, K. D., K. Mohrs, W. Reiley, S. Wittmer, J. E. Kohlmeier, J. E. Pearl, A. M. Cooper, L. L. Johnson, D. L. Woodland, and M. Mohrs. 2008. Cutting edge: T-bet and IL-27R are critical for in vivo IFN-gamma production by CD8 T cells during infection. *J Immunol 180:693-697*.

14. Lugo-Villarino, G., R. Maldonado-Lopez, R. Possemato, C. Penaranda, and L. H. Glimcher. 2003. T-bet is required for optimal production of IFN-gamma and antigen-specific T cell activation by dendritic cells. *Proc Natl Acad Sci U S A 100:7749-7754*.

15. Liu, N., N. Ohnishi, L. Ni, S. Akira, and K. B. Bacon. 2003. CpG directly induces T-bet expression and inhibits IgG1 and IgE switching in B cells. *Nat Immunol 4:687-693*.

16. Werneck, M. B., G. Lugo-Villarino, E. S. Hwang, H. Cantor, and L. H. Glimcher. 2008. T-bet plays a key role in NK-mediated control of melanoma metastatic disease. *J Immunol 180:8004-8010*.

17. Sasaki, Y., K. Ihara, N. Matsuura, H. Kohno, S. Nagafuchi, R. Kuromaru, K. Kusuhara, R. Takeya, T. Hoey, H. Sumimoto, and T. Hara. 2004. Identification of a novel type 1 diabetes susceptibility gene, T-bet. *Hum Genet 115:177-184*.

18. Todd, J. A., N. M. Walker, J. D. Cooper, D. J. Smyth, K. Downes, V. Plagnol, R. Bailey, S. Nejentsev, S. F. Field, F. Payne, C. E. Lowe, J. S. Szeszko, J. P. Hafler, L. Zeitels, J. H. Yang, A. Vella, S. Nutland, H. E. Stevens, H. Schuilenburg, G. Coleman, M. Maisuria, W. Meadows, L. J. Smink, B. Healy, O. S. Burren, A. A. Lam, N. R. Ovington, J. Allen, E. Adlem, H. T. Leung, C. Wallace, J. M. Howson, C. Guja, C. Ionescu-Tirgoviste, M. J. Simmonds, J. M. Heward, S. C. Gough, D. B. Dunger, L. S. Wicker, and D. G. Clayton. 2007. Robust associations of four new chromosome regions from genome-wide analyses of type 1 diabetes. *Nat Genet 39:857-864*.

19. Morahan, G., D. Huang, S. I. Ymer, M. R. Cancilla, K. Stephen, P. Dabadghao, G. Werther, B. D. Tait, L. C. Harrison, and P. G. Colman. 2001. Linkage disequilibrium of a type 1 diabetes susceptibility locus with a regulatory IL12B allele. *Nat Genet 27:218-221*.

20. Hultgren, B., X. Huang, N. Dybdal, and T. A. Stewart. 1996. Genetic absence of gamma-interferon delays but does not prevent diabetes in NOD mice. *Diabetes 45:812-817*.

21. Serreze, D. V., C. M. Post, H. D. Chapman, E. A. Johnson, B. Lu, and P. B. Rothman. 2000. Interferon-gamma receptor signaling is dispensable in the development of autoimmune type 1 diabetes in NOD mice. *Diabetes 49:2007-2011*.

22. Serreze, D. V., H. D. Chapman, C. M. Post, E. A. Johnson, W. L. Suarez-Pinzon, and A. Rabinovitch. 2001. Th1 to Th2 cytokine shifts in nonobese diabetic mice: sometimes an outcome, rather than the cause, of diabetes resistance elicited by immunostimulation. *J Immunol 166:1352-1359*.

23. Kanagawa, O., G. Xu, A. Tevaarwerk, and B. A. Vaupel. 2000. Protection of nonobese diabetic mice from diabetes by gene(s) closely linked to IFN-gamma receptor loci. *J Immunol 164:3919-3923*.

24. Leiter, E. H. 2003. The NOD Mouse: A Model for Insulin-Dependent Diabetes Mellitus. In *Current Protocols in Immunology*. John Wiley and Sons.

25. Judkowski, V., C. Pinilla, K. Schroder, L. Tucker, N. Sarvetnick, and D. B. Wilson. 2001. Identification of MHC class II-restricted peptide ligands, including a glutamic acid decarboxylase 65 sequence, that stimulate diabetogenic T cells from transgenic BDC2.5 nonobese diabetic mice. *J Immunol 166:908-917*.

26. Kanagawa, O., A. Militech, and B. A. Vaupel. 2002. Regulation of diabetes development by regulatory T cells in pancreatic islet antigen-specific TCR transgenic nonobese diabetic mice. *J Immunol 168:6159-6164*.

27. Tang, Q., K. J. Henriksen, M. Bi, E. B. Finger, G. Szot, J. Ye, E. L. Masteller, H. McDevitt, M. Bonyhadi, and J. A. Bluestone. 2004. In vitro-expanded antigen-specific regulatory T cells suppress autoimmune diabetes. *J Exp Med 199:1455-1465*.

28. Katz, J. D., B. Wang, K. Haskins, C. Benoist, and D. Mathis. 1993. Following a diabetogenic T cell from genesis through pathogenesis. *Cell 74:1089-1100*.

29. Ishizaki, K., A. Yamada, K. Yoh, T. Nakano, H. Shimohata, A. Maeda, Y. Fujioka, N. Morito, Y. Kawachi, K. Shibuya, F. Otsuka, A. Shibuya, and S. Takahashi. 2007. Th1 and type 1 cytotoxic T cells dominate responses in T-bet overexpression transgenic mice that develop contact dermatitis. *J Immunol 178:605-612*.

30. Lord, G. M., R. M. Rao, H. Choe, B. M. Sullivan, A. H. Lichtman, F. W. Luscinskas, and L. H. Glimcher. 2005. T-bet is required for optimal proinflammatory CD4+ T-cell trafficking. *Blood 106:3432-3439*.

31. Bour-Jordan, H., B. L. Salomon, H. L. Thompson, G. L. Szot, M. R. Bernhard, and J. A. Bluestone. 2004. Costimulation controls diabetes by altering the balance of pathogenic and regulatory T cells. *J Clin Invest 114:979-987*.

32. You, S., G. Slehoffer, S. Barriot, J. F. Bach, and L. Chatenoud. 2004. Unique role of CD4+CD62L+ regulatory T cells in the control of autoimmune diabetes in T cell receptor transgenic mice. *Proc Natl Acad Sci U S A 101 Suppl 2:14580-14585*.

33. Jackson Laboratory. 2009. Verification of markers at known diabetes susceptibility/resistance (Idd) loci. http://type1diabetes.jax.org/gqc_resistance_suceptibility_loci.html.

34. Anderson, M. S., and J. A. Bluestone. 2005. The NOD mouse: a model of immune dysregulation. *Annu Rev Immunol 23:447-485*.

35. Trembleau, S., G. Penna, E. Bosi, A. Mortara, M. K. Gately, and L. Adorini. 1995. Interleukin 12 administration induces T helper type 1 cells and accelerates autoimmune diabetes in NOD mice. *J Exp Med 181:817-821*.

36. Liu, J., and D. I. Beller. 2003. Distinct pathways for NF-kappa B regulation are associated with aberrant macrophage IL-12 production in lupus- and diabetes-prone mouse strains. *J Immunol 170:4489-4496*.

37. Trembleau, S., G. Penna, S. Gregori, H. D. Chapman, D. V. Serreze, J. Magram, and L. Adorini. 1999. Pancreas-infiltrating Th1 cells and diabetes develop in IL-12-deficient nonobese diabetic mice. *J Immunol 163:2960-2968*.

38. Jain, R., D. M. Tartar, R. K. Gregg, R. D. Divekar, J. J. Bell, H. H. Lee, P. Yu, J. S. Ellis, C. M. Hoeman, C. L. Franklin, and H. Zaghouani. 2008. Innocuous IFNgamma induced

by adjuvant-free antigen restores normoglycemia in NOD mice through inhibition of IL-17 production. *J Exp Med 205:207-218*.

39. Boyton, R. J., S. Davies, C. Marden, C. Fantino, C. Reynolds, K. Portugal, H. Dewchand, and D. M. Altmann. 2005. Stat4-null non-obese diabetic mice: protection from diabetes and experimental allergic encephalomyelitis, but with concomitant epitope spread. *Int Immunol 17:1157-1165*.

40. Yang, Z., M. Chen, J. D. Ellett, L. B. Fialkow, J. D. Carter, M. McDuffie, and J. L. Nadler. 2004. Autoimmune diabetes is blocked in Stat4-deficient mice. *J Autoimmun 22:191-200*.

41. Watford, W. T., B. D. Hissong, J. H. Bream, Y. Kanno, L. Muul, and J. J. O'Shea. 2004. Signaling by IL-12 and IL-23 and the immunoregulatory roles of STAT4. *Immunol Rev 202:139-156*.

42. Thieu, V. T., Q. Yu, H. C. Chang, N. Yeh, E. T. Nguyen, S. Sehra, and M. H. Kaplan. 2008. Signal transducer and activator of transcription 4 is required for the transcription factor T-bet to promote T helper 1 cell-fate determination. *Immunity 29:679-690*.

43. Sullivan, B. M., A. Juedes, S. J. Szabo, M. von Herrath, and L. H. Glimcher. 2003. Antigen-driven effector CD8 T cell function regulated by T-bet. *Proc Natl Acad Sci U S A 100:15818-15823*.

44. Maier, L. M., and L. S. Wicker. 2005. Genetic susceptibility to type 1 diabetes. *Curr Opin Immunol 17:601-608*.

45. Ghosh, S., S. M. Palmer, N. R. Rodrigues, H. J. Cordell, C. M. Hearne, R. J. Cornall, J. B. Prins, P. McShane, G. M. Lathrop, L. B. Peterson, and et al. 1993. Polygenic control of autoimmune diabetes in nonobese diabetic mice. *Nat Genet 4:404-409*.

46. Todd, J. A., T. J. Aitman, R. J. Cornall, S. Ghosh, J. R. Hall, C. M. Hearne, A. M. Knight, J. M. Love, M. A. McAleer, J. B. Prins, and et al. 1991. Genetic analysis of autoimmune type 1 diabetes mellitus in mice. *Nature 351:542-547*.

47. McDuffie, M. 2000. Derivation of diabetes-resistant congenic lines from the nonobese diabetic mouse. *Clin Immunol 96:119-130*.

48. Ivakine, E. A., C. J. Fox, A. D. Paterson, S. M. Mortin-Toth, A. Canty, D. S. Walton, K. Aleksa, S. Ito, and J. S. Danska. 2005. Sex-specific effect of insulin-dependent diabetes 4 on regulation of diabetes pathogenesis in the nonobese diabetic mouse. *J Immunol 174:7129-7140*.

49. Grattan, M., Q. S. Mi, C. Meagher, and T. L. Delovitch. 2002. Congenic mapping of the diabetogenic locus Idd4 to a 5.2-cM region of chromosome 11 in NOD mice: identification of two potential candidate subloci. *Diabetes 51:215-223*.

50. Salomon, B., D. J. Lenschow, L. Rhee, N. Ashourian, B. Singh, A. Sharpe, and J. A. Bluestone. 2000. B7/CD28 costimulation is essential for the homeostasis of the CD4+CD25+ immunoregulatory T cells that control autoimmune diabetes. *Immunity 12:431-440*.

Figures/Tables

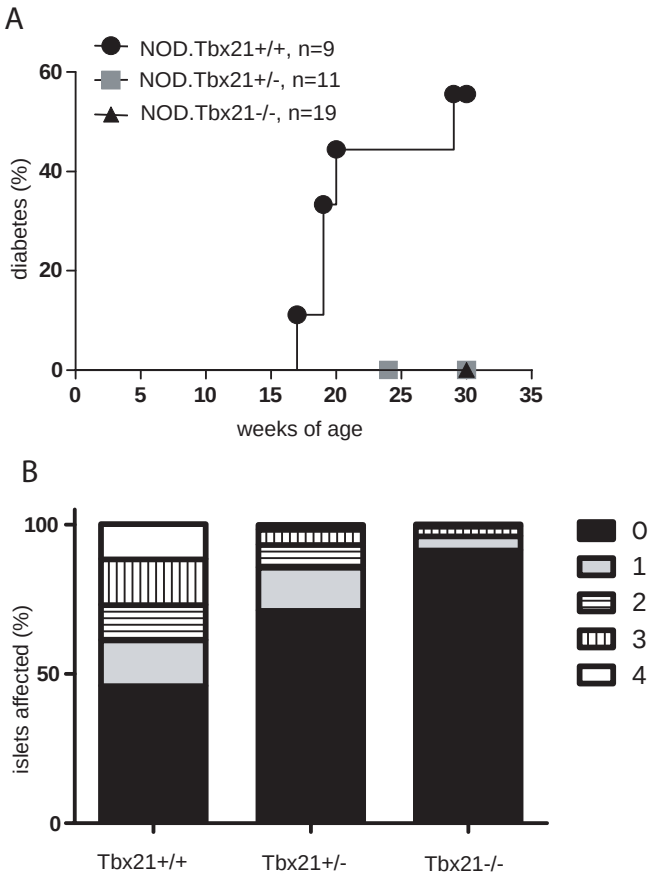

FIGURE 3.1. *Tbx21* deficiency protects NOD mice from insulitis and diabetes. A, Female NOD.*Tbx21*$^{-/-}$ mice and their $^{+/-}$ and $^{+/+}$ littermates were followed for diabetes for 30 weeks. B, Mice from the above cross were sacrificed for histopathological analysis of the pancreas at 12 weeks of age. Grade 0, no insulitis; grade 1, perivascular and periductal mononuclear cell infiltration outside of islet perimeter; grade 2, mononuclear cell penetration of up to 25% of islet; grade 3, mononuclear cell penetration of up to 75% of islet; grade 4, islet destruction with less than 20% of islet mass remaining. Results are from at least 100 islets from 4 animals per genotype.

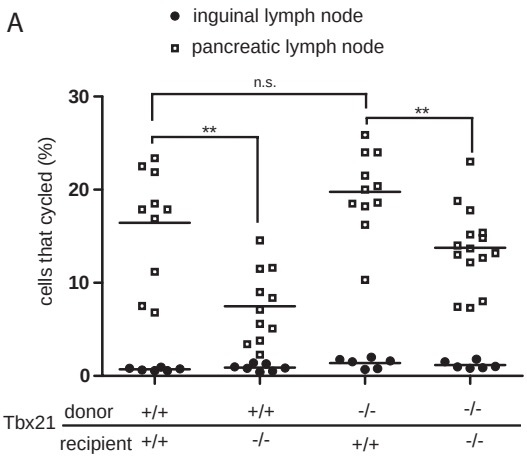
A
inguinal lymph node
pancreatic lymph node
n.s.
**
**
cells that cycled (%)
30
20
10
0
Tbx21 donor +/+ +/+ -/- -/-
recipient +/+ -/- +/+ -/-

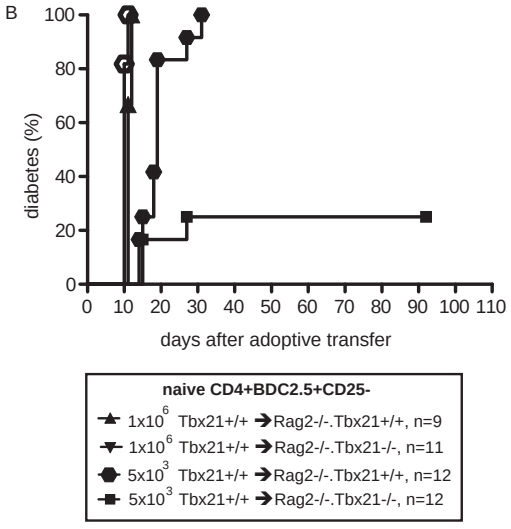
B
diabetes (%)
100
80
60
40
20
0
0 10 20 30 40 50 60 70 80 90 100 110
days after adoptive transfer
naive CD4+BDC2.5+CD25-
1x10^6 Tbx21+/+ → Rag2-/-.Tbx21+/+, n=9
1x10^6 Tbx21+/+ → Rag2-/-.Tbx21-/-, n=11
5x10^3 Tbx21+/+ → Rag2-/-.Tbx21+/+, n=12
5x10^3 Tbx21+/+ → Rag2-/-.Tbx21-/-, n=12

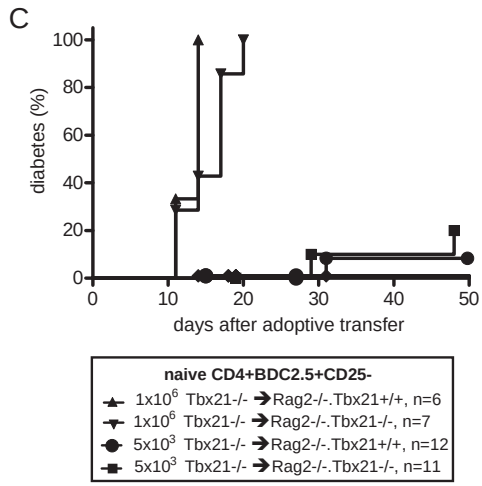
C
diabetes (%)
100
80
60
40
20
0
0 10 20 30 40 50
days after adoptive transfer
naive CD4+BDC2.5+CD25-
1x10^6 Tbx21-/- → Rag2-/-.Tbx21+/+, n=6
1x10^6 Tbx21-/- → Rag2-/-.Tbx21-/-, n=7
5x10^3 Tbx21-/- → Rag2-/-.Tbx21+/+, n=12
5x10^3 Tbx21-/- → Rag2-/-.Tbx21-/-, n=11

FIGURE 3.2

FIGURE 3.2. *Tbx21* is necessary in both T cells and APCs in an adoptive transfer model of diabetes. A, CD4+CD25$^-$ BDC2.5 TCR transgenic T cells from *Tbx21*$^{-/-}$ and *Tbx21*$^{+/+}$ mice were labeled with CFSE. The cells were collected, recounted, and 1×10^6 were adoptively transferred into NOD or NOD.*Tbx21*$^{-/-}$ recipients. After 72 hours, pancreatic lymph nodes from the recipient mice were harvested and polyclonal lymph node cells were stained for CD4 and the BDC2.5 TCR. Each data point is an individual mouse, and the line is the mean of all mice in a group. ** indicates a p-value of <0.01 using a 2-tailed unpaired T test. n.s. indicates that p>0.05. B, 1×10^6 or 5×10^3 freshly isolated CD4+CD25$^-$ BDC2.5 transgenic T cells from *Tbx21*$^{+/+}$ mice were adoptively transferred into NOD.*Rag2*$^{-/-}$.*Tbx21*$^{-/-}$ or NOD.*Rag2*$^{-/-}$.*Tbx21*$^{+/+}$ mice. The mice were followed for diabetes incidence. Results are from two or three independent experiments. C, 1×10^6 or 5×10^3 freshly isolated CD4+CD25$^-$ BDC2.5 transgenic T cells from *Tbx21*$^{-/-}$ mice were adoptively transferred into NOD.*Rag2*$^{-/-}$.*Tbx21*$^{-/-}$ or NOD.*Rag2*$^{-/-}$.*Tbx21*$^{+/+}$ mice. The mice were followed for diabetes incidence. Results are from three independent experiments.

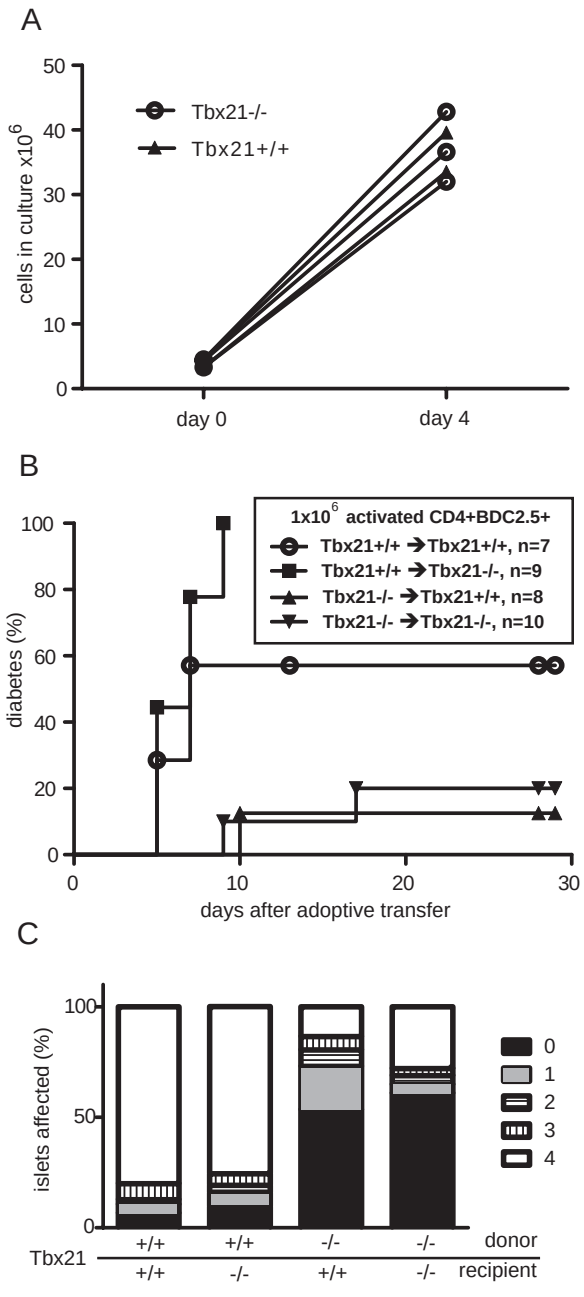

FIGURE 3.3. Defective adoptive transfer of diabetes with activated *Tbx21*$^{-/-}$ BDC2.5 TCR transgenic T cells. A, CD4+CD25^{-} BDC2.5 transgenic T cells from *Tbx21*$^{-/-}$ and *Tbx21*$^{+/+}$ mice were activated in-vitro using irradiated T-depleted NOD splenocytes and the Acp31 mimeotope peptide. Cells in culture were counted before initial activation and again immediately before adoptive transfer. B, 1×10^{6} of these activated BDC2.5 TCR transgenic cells were transferred into age-matched non-diabetic NOD or NOD.*Tbx21*$^{-/-}$ animals, which were followed for diabetes. Diabetes incidence of *Tbx21*$^{-/-}$ and *Tbx21*$^{+/+}$ recipients transferred with *Tbx21*$^{+/+}$ BDC2.5 T cells is not significantly different (log rank test, p=0.10). C, Alternatively, some of the adoptively transferred mice were sacrificed at day 5 post-transfer for histopathological analysis of pancreatic islet inflammation. Results are from two independent experiments.

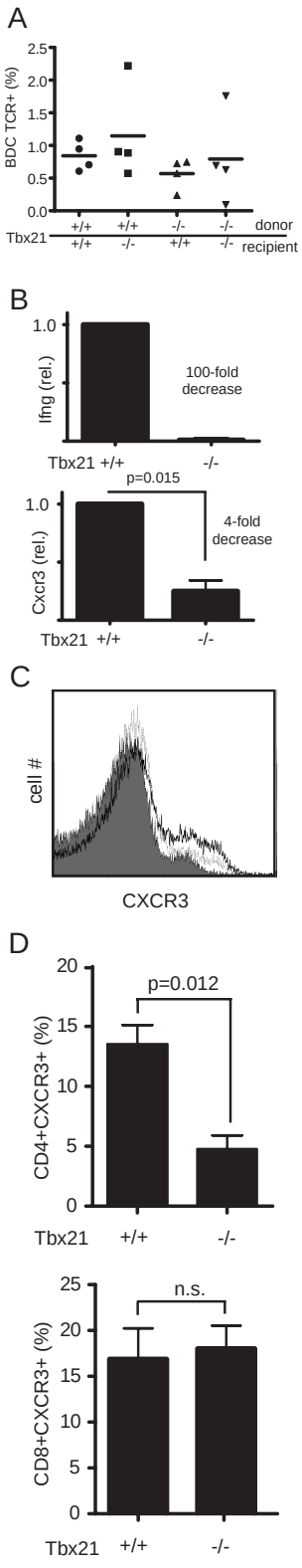

FIGURE 3.4. *Tbx21* deficient BDC2.5 TCR transgenic T cells are defective in IFN-γ production and *Cxcr3* expression. A, Pancreatic lymph nodes were harvested from mice described in Figure 3C at day 5 after adoptive transfer of activated BDC2.5 TCR transgenic T cells. Lymph node cells were stained for the BDC2.5 TCR. Percentages indicated are out of total CD4+ cells. B, CD4+CD25^{-} BDC2.5 TCR transgenic T cells from *Tbx21*$^{-/-}$ and *Tbx21*$^{+/+}$ mice were activated *in-vitro* by using irradiated T-depleted NOD splenocytes and the Acp31 mimeotope peptide. Total cellular RNA was collected 4 days after activation and assayed by real-time PCR for levels of *Ifng* and *Cxcr3* mRNA. Expression of each gene in *Tbx21*$^{+/+}$ samples was indexed to 1. Data was pooled from three independent experiments and analyzed with a one-sample T test. C, Freshly isolated CD4+ splenocytes were stained using a polyclonal Ab for cell surface expression of CXCR3 protein and measured by flow cytometry. Gray tracing is no primary Ab; dotted line is *Tbx21*$^{-/-}$ splenocytes; and dark line is *Tbx21*$^{+/+}$ splenocytes. Data is representative of three experiments. D, Quantitative analysis of CXCR3^{+} cells in freshly isolated splenocytes in the total CD4+ population (top panel) and the CD8+ population (bottom panel). Data was pooled from three independent experiments and analyzed with a 2-tailed upaired T test. Error bars represent the standard error of the mean.

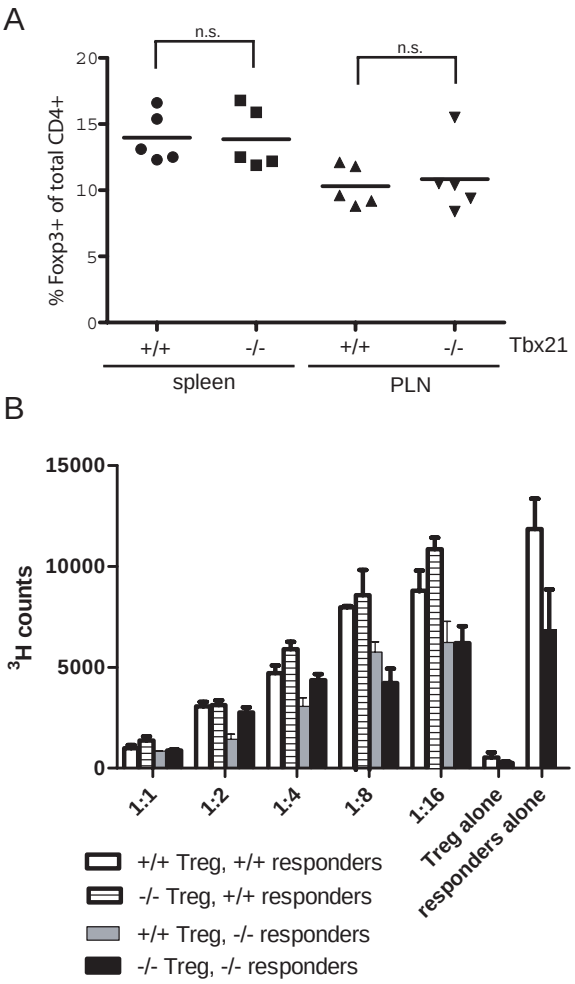

FIGURE 3.5. *Tbx21*-deficient mice have normal numbers of functional Tregs. A, Splenocytes and pancreatic lymph node cells from NOD and NOD.*Tbx21*$^{-/-}$ mice were stained for CD4 and FOXP3. Each data point represents an individual mouse. Groups were compared with an unpaired two-tailed T test. n.s. is not statistically significant. B, CD4+CD25$^+$CD62L$^+$ regulatory T cells were purified by FACS and titrated in a suppression assay with CD4+CD25$^-$ responder cells. Responders were activated with soluble anti-CD3 and irradiated syngeneic splenocytes. A 1:1 ratio of Tregs to responders has 5×10^4 of each cell type. Data is representative of three independent experiments. Error bars are standard error of the mean.

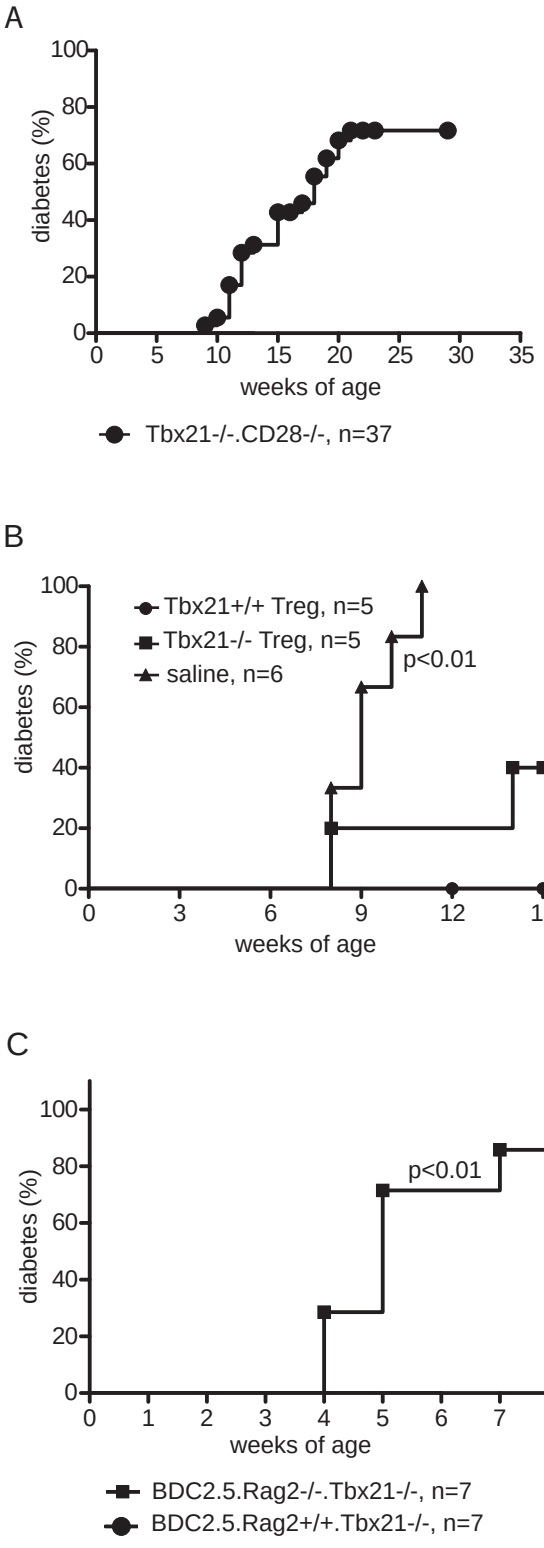

FIGURE 3.6. Tregs are required to prevent diabetes in *Tbx21*$^{-/-}$ mice. A, NOD.*Tbx21*$^{-/-}$.Cd28$^{-/-}$ mice were followed for spontaneous diabetes incidence. B, *NOD.Cd28*$^{-/-}$ mice were treated at 7 weeks of age with 3×10^5 *in vitro* expanded Tregs from either BDC2.5 *Tbx21*$^{+/+}$ or BDC2.5 *Tbx21*$^{-/-}$ mice, or with saline as a control. The mice were then followed for diabetes incidence. The survival curve of mice that received *Tbx21*$^{-/-}$ Tregs is significantly different from the survival curve of the mice that did not receive any Tregs (log rank test, $p<0.01$). C, NOD.BDC2.5.*Rag2*$^{-/-}$.*Tbx21*$^{-/-}$ mice were followed for diabetes incidence.

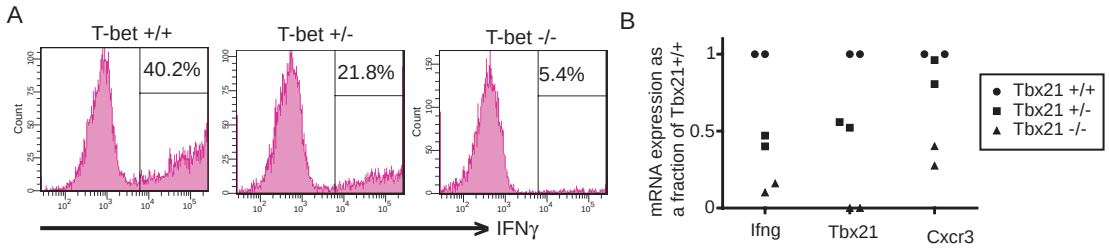

SUPPLEMENTAL FIGURE 3.1. CD4+ T cells from *Tbx21*$^{+/-}$ mice express half as much IFNγ and *Tbx21* as *Tbx21*$^{+/+}$ cells. A, CD4+ T cells were purified and activated with plastic-bound anti-CD3 and anti-CD28 for 6 days in Th1-skewing conditions (20 ng/mL IL-12, 20 µg/mL anti-IL-4, and 100 U/mL IL-2). The cells were re-stimulated for 3 hours with PMA (10 ng/mL) and ionomycin (0.5 µM) in the presence of monensin (3 µM) before fixation and staining for intracellular IFN-γ. B, RNA was extracted from the cells after primary activation described in part A and Taqman real-time PCR assays were performed. The 18S ribosomal RNA was used as an endogenous control. Each data point in a given gene's column represents an independent experiment.

	Name	Chr	Position	NOD.T-bet KO allele 1	allele 2
	rs3701734	11	41080566	N	N
	rs13481009	11	46281254	N	N
	rs6199956	11	50498109	N	N
	rs3697686	11	58293180	N	N
	rs3711357	11	61178207	N	N
	rs13481061	11	62718268	N	N
	D11Mit339	11	63806459		
JAX Idd4	rs13481071	11	64926468	N	N
	rs13481084	11	68496175	N	N
	D11Mit298	11	69340023		
	D11Mit219	11	72135165	N	N
	rs13481094	11	72560077	N	N
	D11Nds1	11	74677336		
	D11Mit322	11	76395518	S	S
	rs13481127	11	83140519	S	S
	rs3661657	11	84460360	S	S
	rs3719581	11	86686874	S	S
	rs13481170	11	95449190	S	S
	T-bet	11	96959386	S	S
	T-bet	11	96976589	S	S
	Stat5b	11	100642045	S	S

SUPPLEMENTAL TABLE 3.1. Genetic markers on the distal portion of chromosome 11 in the NOD.*Tbx21*$^{-/-}$ mouse. A combination of SNPs, microsatellite markers, and coding sequence polymorphisms were used to determine the border of the genomic region derived from the 129/S6SvEvTac strain, which was used to derived the TC1 ES cells used to make the *Tbx21*$^{-/-}$ mouse (11). N signifies a NOD-derived allele and S signifies a 129/S6SvEvTac-derived allele. The markers used by the Jackson Laboratory to genotype for the *Idd4* locus are highlighted in gray and labeled "JAX Idd4." (33) The *Tbx21* locus is also highlighted in gray.

Chapter 4: General Discussion

The various phenotypes and functions of CD4+ T cells are controlled by many things: the T cell's developmental history, the cytokines in the cell's immediate microenvironment, and the quality of antigen-specific signals that the cell receives. The work described in this dissertation is an attempt to understand how these inputs are integrated to drive the expression of specific transcription factors. These transcription factors, in turn, are critical for the normal functioning of CD4+ effector T cells. We set out to test two hypotheses: that Tbx21 would be required for normal autoimmune diabetes in the NOD mouse, and that the transcriptional phenotype of CD28 costimulation requires the function of one or more CD28-induced transcription factors. In this section, the key findings of chapters 2 and 3 are reviewed and related to the original hypotheses. The results are discussed in the context of the broader field of research on the diversity of phenotype and function of CD4+ T effector cells. Where appropriate, future experiments are discussed that may answer the many outstanding questions raised by this dissertation.

CD28 and Bhlhe40 in T cell activation

CD4+ T cells require two signals for activation: an antigen-specific signal delivered through the T cell receptor and a costimulatory signal. Engagement of the CD28 receptor on T cells by its ligands CD80 and CD86 provides the most important costimulatory signal for naive CD4+ T cells. CD28 signals drive T cell proliferation, protect the cell from apoptosis, and support IL-2 production (reviewed in 1). The importance of CD28 signals to T cell activation was first shown more than 25 years ago with the demonstration that monoclonal antibodies against CD28 promote T cell proliferation (2) and increase IL-2 production by increasing mRNA stability (3)(4). Work by Weiss and colleagues demonstrated that the CD28 response element, an enhancer element in the IL-2 locus similar to a kappa-B motif, is critical for the expression of IL-2 after CD28 costimulation (5).

Further work on the mechanism of CD28 costimulation has shown that CD28 ligation amplifies TCR signals by recruiting PKC-theta to the immunological synapse (6), which augments the PI3 kinase/Akt pathway (7). CD28 also recruits the guanine nucleotide exchange factor Vav, the adaptor protein SLP-76 (8, 9), and the actin binding protein filamin-A to the immunological synapse. This recruitment facilitates the formation of lipid rafts and amplifies TCR signaling (10). These signals may be critical to inducing a unique set of transcription factors that prevent anergy induced by unopposed calcium signals (11). Thus, small differences in signals at the cell surface may be magnified into large differences in transcription factor activity in the nucleus. Alternatively, CD28 signals may work by preventing the export of NFAT transcription factors from the nucleus (12). CD28 also functions by blocking anergy induction mediated by E3 ubiquitin ligases such as Cbl-b (13). T cells from mice deficient for Cbl-b produce large quantities of IL-2 even in the absence of costimulation (14).

Despite these advances in understanding the membrane-proximal signaling events downstream of CD28 costimulation, transcription factors that are uniquely important for CD28 costimulation have not been described. NF-kappaB family members, including c-Rel might be important for IL-2 production after T cell activation (15-17). However, these transcription factors alone cannot explain the complex transcriptional changes that occur after CD28 costimulation. Further, the authors of a pair of microarray studies that probed the transcriptional response to CD28 costimulation argue that CD28 costimulation principally amplifies the transcriptional changes initiated by TCR ligation (18, 19). Thus, these data support the hypothesis that CD28 costimulation provides a mostly “quantitative” signal to amplify the transcriptional program initiated by TCR ligation (20).

The global mRNA expression analyses described in this dissertation suggest that the current view of CD28 costimulation as providing quantitative support to the TCR signal may be more complex that originally envisioned. In chapter 2, we described microarray data that show a

clearly qualitative effect of CD28 costimulation on T cell activation. We generated genome-wide mRNA expression profiles from naive human CD4+ T cells activated with or without costimulation via CD28. Using this data, we argue that the debate over whether CD28 costimulation affects gene expression in a predominantly quantitative or qualitative way is a result of differing experimental approaches. In particular, previously published microarray studies have used mixed populations of either whole primary CD4+ cells (18) or unfractionated primary T cells (19). Microarray results from activation experiments using mixed populations of cells are difficult to interpret because the cells with little or no dependence of CD28 costimulation for activation would give a "quantitative" profile whereas the CD28-dependent cells would be expected to give a "qualitative profile." Using carefully separated populations of highly CD28-dependent cells (primary human CD4+CD45RA+ T cells), we showed that CD28 costimulation has mostly quantitative effects on global gene expression at early time points after activation (4 hours), but strongly qualitative effects on transcription at later time points (24 hours).

What is responsible for the strongly qualitative effects of CD28 costimulation at the 24 hour time point? We hypothesized that one or more transcription factors would be necessary to induce and maintain the transcriptional phenotype of a costimulated cell. By analogy with T effector cell subsets that have lineage-specifying transcription factors that are highly expressed in those subsets, we looked for transcription factors whose expression was upregulated more than 5-fold by CD28 costimution compared to TCR ligation alone at both 4 and 24 hours after activation. This short list of genes included *BHLHE40*, a basic helix-loop-helix (BHLH) transcription factor which has been previously implicated in T cell function, but not specifically in CD28 costimulation (21). In chapter 2, we showed that *BHLHE40* is critical for the transcriptional response to CD28 costimulation in both Jurkat T cells and primary mouse CD4+ T cells. Importantly, we showed that the effects of Bhlhe40 deficiency impact specifically on CD28 costimulation-dependent gene expression. For example, Jurkat cells with BHLHE40 knocked-

down by an shRNA or *Bhlhe40 -/-* primary mouse CD4+ cells both upregulate CD69 to normal levels after activation with anti-CD3 and anti-CD28, but IL-2 expression is decreased at least 50% compared to the Bhlhe40-sufficient controls. Bhlhe40 has a closely related homolog, Bhlhe41, which has an identical BHLH DNA binding domain (Figure 4.1). These two transcription factors are already known to work together in the regulation of circadian rhythm in mice (22). Thus, further work will focus on *in vivo* results of Bhlhe40 deficiency and on any possible roles that Bhlhe41 may play in CD28 costimulation. Mouse lines that have null mutations in both Bhlhe40 and Bhlhe41 will be used for *in vitro* and *in vivo* experiments to test whether these two transcription factors overlap in their role supporting CD28 costimulation.

Tbx21 (T-bet) and the making of Th1 cells

Since the first description of the different roles of CD4+ and CD8+ T cells by Cantor and Boyce in 1975 (23), the diversity of T cell phenotypes and the lineage relationships between those subsets has become a major focus in immunology research. Important milestones in the understanding of CD4+ helper T cells include the description of distinct Th1 and Th2 phenotypes by Mossman and Coffman (24) and the subsequent discovery of Tbx21 (for Th1) and Gata3 (for Th2) as the lineage-specifying transcription factors for these T cell subsets (25)(26). Since these seminal discoveries, a large variety of other T cell subsets (e.g. Th17, Th9, Th22, nTreg, Tfh) and, in some cases, their lineage-specifying transcription factors have been described (27, 28,29,30, 31,32). For Th1 cells, the lineage specifying transcription factor is Tbx21(25), with its homolog Eomesodermin playing an important role in CD8+ T cell function during Th1 responses (33)(34).

What subsets of CD4+ T cells are responsible for autoimmune diseases such as Type 1 diabetes? To test whether Tbx21, and by extension, Th1-skewed CD4+ T cells are important in autoimmune diabetes, we backcrossed the non-obese diabetic (NOD) mouse to the *Tbx21 -/-* animal. These *NOD.Tbx21 -/-* mice were completely protected from diabetes. Furthermore, these

animals were also free from mononuclear cell infiltration in their islets of Langerhans. Proliferation of CD4+ T cells specific for an islet antigen was decreased in the pancreatic lymph nodes of *Tbx21 -/-* animals, compared to control (Figure 3.2A), implying that there is a defect in initial priming of diabetogenic T cells in these animals. Although TCR transgenic *Tbx21 -/-* T cells can cause disease in adoptive transfer models of diabetes, they are much less efficient at causing disease than *Tbx21 +/+* cells when transferred at low numbers into a recipient animal. Taken together, these findings demonstrate that Tbx21 is necessary for effector phenotypes beyond production of IFN-γ, the signature Th1 cytokine. Conversely, the *Tbx21-/-* cells are fully competent to cause disease in adoptive transfer models, showing that these T cells can be pathogenic in the absence of attaining a "full Th1" phenotype.

These results have important implications for therapies that block one or more cytokines thought to be involved in the pathogenesis of autoimmune or autoinflammatory disease. As the work described above shows, blocking the characteristic cytokine of a particular T effector cell subset may not block the pathogenic potential of T cells. An important question for future study is how much the phenotype of pathogenic *Tbx21 -/-* T cells mirrors a classic Th1 cell. There is evidence that the differentiation of some cell types, such as Tregs, is initiated even in the absence of the lineage-specifying transcription factor Foxp3 (35). Further, many of the targets of lineage specifying transcription factors may not be specific to a particular subset or T cell phenotype. A genome-wide ChIP binding study shows that Tbx21 binds more than 800 gene loci in primary Th1-skewed T cells. Tbx21 expression in Th1 cells often occurred simultaneously with expression of Gata3, the Th2 lineage specifying factor. Importantly, these two transcription factors shared targets: 39% of genes that bound Tbx21 in Th1 cells were simultaneously bound to Gata3 (36). These surprising findings show that the expression of a lineage-specifying transcription factor has different phenotypic results depending on the context in which a cell has developed. Thus, microarray studies on activated *Tbx21 -/-* T cells may elucidate the specific

genetic program controlled uniquely by Tbx21 and not by other transcription factors. Such array data could then be compared to the ChIP data in (36) to determine which Th1-associated genes are completely Tbx21-dependent in CD4+ T cells (such as *Ifng*) and which genes are only partially Tbx21 dependent.

Outlook

The work described in this dissertation contributes to an emerging picture of complexity of the phenotypes of CD4+ effector T cells. This complexity has led some immunologists to question the usefulness of the existing conceptual framework used to described CD4+ T cell phenotypes. For example, William E. Paul and John J. O'Shea wrote a recent review questioning whether the existing T cell lineages can be defined clearly given the instability of expression of certain lineage-defining cytokines and transcription factors (37). In particular, the authors cite the case of Tfh cells that express the lineage-specifying transcription factor Bcl6 (32) but still have an uncertain lineage relationship with other subsets. For example, these T follicular helper (Tfh) cells can also express cytokines that are characteristic of Th1 and Th2 subsets(38, 39, 40). Similarly, human Treg cells can express IFN-γ (41), and Tbx21 may be important for Treg homing to sites of Th1 mediated inflammation (42). In the extreme, such overlap of subset phenotypes could lead to complete loss of a functional phenotype. For example, Tregs that have lost their regulatory phenotype due to Foxp3 downregulation subsequently start producing IFN-γ and gain the ability to cause autoimmune disease (43). Similarly, highly purified Th17-skewed autoreactive T cells convert to Th1 cells when transferred into a lymphopenic mouse (44). Thus, the "map" of CD4+ T cell differentiation is probably much more complex than the traditional simple arrow diagrams suggest.

The data presented in chapter 3 on the role of Tbx21 in autoimmune diabetes shows that although Tbx21 is necessary for spontaneous disease, *Tbx21 -/-* CD4+ T cells are still highly pathogenic and cause rapid autoimmune diabetes under some circumstances. Are these cells still

Th1 cells, even though they do not produce IFN-γ? As Paul and O'Shea point out, the production of a specific cytokine such as IFN-γ may be neither necessary nor sufficient to place a given cytokine into a particular subset (37). Rather, cytokine production may be better described in probabilistic terms, depending on the levels of various transcription factors in the nucleus of a cell at a given time. Furthermore, the phenotype of Th1 cells is likely controlled not only by Tbx21 expression, but also by other transcription factors such as Runx3(45) and Hlx (46). Thus, it may be an oversimplification to designate type 1 diabetes a Th1-driven disease, because both IFN-γ null (47) and IL-12 null (48) NOD mice develop normal, spontaneous diabetes. As we showed in chapter 3, Tbx21 is necessary in both T cells and antigen presenting cells for maximal disease in adoptive transfer models. The role of Tbx21 in non-T cells is an important reminder that T cells develop in response to complex microenvironments and interactions with antigen presenting cells. Further studies with a floxed allele of Tbx21 will allow for tissue-specific gene ablation to more precisely piece apart the specific contributions of Tbx21 to spontaneous diabetes.

The transcription-factor-centered view of T cell phenotypes may also be helpful in understanding the transcriptional responses to CD28 costimulation. However, it is unlikely that any one transcription factor directs the complex transcriptional profile of a cell that has received CD28 costimulation. More likely, CD28 costimulation leads to the recruitment of a large number of transcription factors to the nucleus, and the specific balance of different transcription factors determines the overall transcriptional phenotype of the cell (11). Thus, further work with Bhlhe40 and its homolog Bhlhe41 may lead to a better understanding of how these factors contribute to the transcriptional phenotype of a naive T cell that is activated with CD28 costimulation. In particular, ChIP experiments to identify direct targets of these transcription factors before and after activation with CD28 costimulation might yield insight into their roles. Combined with further expression data on primary T cells lacking Bhlhe40 and Bhlhe41, future work may yield a more complete picture of the specific gene expression changes that occur with CD28

costimulation. These studies might also be relevant to regulatory T cell biology, because Tregs are highly CD28-dependent (49). Previous data has also shown that Bhlhe40 is highly expressed in Tregs compared to non-Tregs (35). Thus, Bhlhe40 may have roles in both effector T cell and regulatory T cell function through its role in CD28 costimulation.

How much information must be known about a CD4+ T cell to be able to assign it to a given "subset" or functional phenotype? Traditionally, cell surface markers have been used because they are easily measured on a per cell basis by flow cytometry. However, cell surface markers in many cases only approximate the true developmental state of a T cell. Transcription factors may be more accurate measures of cell phenotype, but they are more difficult to measure and, as described above, their presence or absence affects a cell's phenotype in a highly context-dependent manner. Thus, future work on understanding CD4+ T cell diversity will need to describe a complex multi-dimensional landscape of phenotypes and the possible routes of differentiation between them. Complicating this view, the complexity of different phenotypes may mirror the complexity of the particular microenvironment and antigen stimulus. Such complex relationships between phenotypes have been described in highly artificial systems, such as variations in apoptosis of an epithelial cell line stimulated with various concentrations of TNF, EGF, and insulin (50). Microarrays and ChIP-seq technology (51) have already greatly expanded the understanding of the transcriptional status of different types of T cells. Due to the complexity of T cell phenotypes and microenvironments, new technologies for tracking and measuring gene expression in single cells in vivo will likely be necessary to make a more accurate map of the dynamic phenotypic diversity of CD4+ T cells.

References

1. Lenschow, D. J., T. L. Walunas, and J. A. Bluestone. 1996. CD28/B7 system of T cell costimulation. *Annu. Rev. Immunol.* 14: 233-258.

2. Gmunder, H. and W. Lesslauer. 1984. A 45-kDa human T-cell membrane glycoprotein functions in the regulation of cell proliferative responses. *Eur. J. Biochem.* 142: 153-160.

3. Ledbetter, J. A., P. J. Martin, C. E. Spooner, D. Wofsy, T. T. Tsu, P. G. Beatty, and P. Gladstone. 1985. Antibodies to Tp67 and Tp44 augment and sustain proliferative responses of activated T cells. *J. Immunol.* 135: 2331-2336.

4. Weiss, A., B. Manger, and J. Imboden. 1986. Synergy between the T3/antigen receptor complex and Tp44 in the activation of human T cells. *J. Immunol.* 137: 819-825.

5. Fraser, J. D., B. A. Irving, G. R. Crabtree, and A. Weiss. 1991. Regulation of interleukin-2 gene enhancer activity by the T cell accessory molecule CD28. *Science* 251: 313-316.

6. Yokosuka, T., W. Kobayashi, K. Sakata-Sogawa, M. Takamatsu, A. Hashimoto-Tane, M. L. Dustin, M. Tokunaga, and T. Saito. 2008. Spatiotemporal regulation of T cell costimulation by TCR-CD28 microclusters and protein kinase C theta translocation. *Immunity* 29: 589-601.

7. Kane, L. P., P. G. Andres, K. C. Howland, A. K. Abbas, and A. Weiss. 2001. Akt provides the CD28 costimulatory signal for up-regulation of IL-2 and IFN-gamma but not TH2 cytokines. *Nat. Immunol.* 2: 37-44.

8. Rudd, C. E. and M. Raab. 2003. Independent CD28 signaling via VAV and SLP-76: a model for in trans costimulation. *Immunol. Rev.* 192: 32-41.

9. Michel, F., G. Mangino, G. Attal-Bonnefoy, L. Tuosto, A. Alcover, A. Roumier, D. Olive, and O. Acuto. 2000. CD28 utilizes Vav-1 to enhance TCR-proximal signaling and NF-AT activation. *J. Immunol.* 165: 3820-3829.

10. Tavano, R., R. L. Contento, S. J. Baranda, M. Soligo, L. Tuosto, S. Manes, and A. Viola. 2006. CD28 interaction with filamin-A controls lipid raft accumulation at the T-cell immunological synapse. *Nat. Cell Biol.* 8: 1270-1276.

11. Macian, F., F. Garcia-Cozar, S. H. Im, H. F. Horton, M. C. Byrne, and A. Rao. 2002. Transcriptional mechanisms underlying lymphocyte tolerance. *Cell* 109: 719-731.

12. Pan, M., M. M. Winslow, L. Chen, A. Kuo, D. Felsher, and G. R. Crabtree. 2007. Enhanced NFATc1 nuclear occupancy causes T cell activation independent of CD28 costimulation. *J. Immunol.* 178: 4315-4321.

13. Zhang, J., T. Bardos, D. Li, I. Gal, C. Vermes, J. Xu, K. Mikecz, A. Finnegan, S. Lipkowitz, and T. T. Glant. 2002. Cutting edge: regulation of T cell activation threshold by CD28 costimulation through targeting Cbl-b for ubiquitination. *J. Immunol.* 169: 2236-2240.

14. Chiang, Y. J., H. K. Kole, K. Brown, M. Naramura, S. Fukuhara, R. J. Hu, I. K. Jang, J. S. Gutkind, E. Shevach, and H. Gu. 2000. Cbl-b regulates the CD28 dependence of T-cell activation. *Nature* 403: 216-220.

15. Rao, S., S. Gerondakis, D. Woltring, and M. F. Shannon. 2003. c-Rel is required for chromatin remodeling across the IL-2 gene promoter. *J. Immunol.* 170: 3724-3731.

16. Sanchez-Valdepenas, C., A. G. Martin, P. Ramakrishnan, D. Wallach, and M. Fresno. 2006. NF-kappaB-inducing kinase is involved in the activation of the CD28 responsive element through

phosphorylation of c-Rel and regulation of its transactivating activity. *J. Immunol.* 176: 4666-4674.

17. Kontgen, F., R. J. Grumont, A. Strasser, D. Metcalf, R. Li, D. Tarlinton, and S. Gerondakis. 1995. Mice lacking the c-rel proto-oncogene exhibit defects in lymphocyte proliferation, humoral immunity, and interleukin-2 expression. *Genes Dev.* 9: 1965-1977.

18. Riley, J. L., M. Mao, S. Kobayashi, M. Biery, J. Burchard, G. Cavet, B. P. Gregson, C. H. June, and P. S. Linsley. 2002. Modulation of TCR-induced transcriptional profiles by ligation of CD28, ICOS, and CTLA-4 receptors. *Proc. Natl. Acad. Sci. U. S. A.* 99: 11790-11795.

19. Diehn, M., A. A. Alizadeh, O. J. Rando, C. L. Liu, K. Stankunas, D. Botstein, G. R. Crabtree, and P. O. Brown. 2002. Genomic expression programs and the integration of the CD28 costimulatory signal in T cell activation. *Proc. Natl. Acad. Sci. U. S. A.* 99: 11796-11801.

20. Acuto, O. and F. Michel. 2003. CD28-mediated co-stimulation: a quantitative support for TCR signalling. *Nat. Rev. Immunol.* 3: 939-951.

21. Sun, H., B. Lu, R. Q. Li, R. A. Flavell, and R. Taneja. 2001. Defective T cell activation and autoimmune disorder in Stra13-deficient mice. *Nat. Immunol.* 2: 1040-1047.

22. Honma, S., T. Kawamoto, Y. Takagi, K. Fujimoto, F. Sato, M. Noshiro, Y. Kato, and K. Honma. 2002. Dec1 and Dec2 are regulators of the mammalian molecular clock. *Nature* 419: 841-844.

23. Cantor, H. and E. A. Boyse. 1975. Functional subclasses of T lymphocytes bearing different Ly antigens. *The Journal of Experimental Medicine* 141: 1376.

24. Mosmann, T. R., H. Cherwinski, M. W. Bond, M. A. Giedlin, and R. L. Coffman. 1986. Two types of murine helper T cell clone. I. Definition according to profiles of lymphokine activities and secreted proteins. *J. Immunol.* 136: 2348-2357.

25. Szabo, S. J., S. T. Kim, G. L. Costa, X. Zhang, C. G. Fathman, and L. H. Glimcher. 2000. A novel transcription factor, T-bet, directs Th1 lineage commitment. *Cell* 100: 655-669.

26. Zheng, W. and R. A. Flavell. 1997. The transcription factor GATA-3 is necessary and sufficient for Th2 cytokine gene expression in CD4 T cells. *Cell* 89: 587-596.

27. Zhu, J. and W. E. Paul. 2008. CD4 T cells: fates, functions, and faults. *Blood* 112: 1557-1569.

28. Fontenot, J. D., M. A. Gavin, and A. Y. Rudensky. 2003. Foxp3 programs the development and function of CD4+CD25+ regulatory T cells. *Nat. Immunol.* 4: 330-336.

29. Ivanov, I. I., B. S. McKenzie, L. Zhou, C. E. Tadokoro, A. Lepelley, J. J. Lafaille, D. J. Cua, and D. R. Littman. 2006. The orphan nuclear receptor RORgammat directs the differentiation program of proinflammatory IL-17+ T helper cells. *Cell* 126: 1121-1133.

30. Eyerich, S., K. Eyerich, D. Pennino, T. Carbone, F. Nasorri, S. Pallotta, F. Cianfarani, T. Odorisio, C. Traidl-Hoffmann, H. Behrendt, S. R. Durham, C. B. Schmidt-Weber, and A. Cavani. 2009. Th22 cells represent a distinct human T cell subset involved in epidermal immunity and remodeling. *J. Clin. Invest.* 119: 3573-3585.

31. Veldhoen, M., C. Uyttenhove, J. van Snick, H. Helmby, A. Westendorf, J. Buer, B. Martin, C. Wilhelm, and B. Stockinger. 2008. Transforming growth factor-beta 'reprograms' the differentiation of T helper 2 cells and promotes an interleukin 9-producing subset. *Nat. Immunol.* 9: 1341-1346.

32. Yu, D., S. Rao, L. M. Tsai, S. K. Lee, Y. He, E. L. Sutcliffe, M. Srivastava, M. Linterman, L. Zheng, N. Simpson, J. I. Ellyard, I. A. Parish, C. S. Ma, Q. J. Li, C. R. Parish, C. R. Mackay, and C. G. Vinuesa. 2009. The transcriptional repressor Bcl-6 directs T follicular helper cell lineage commitment. *Immunity* 31: 457-468.

33. Intlekofer, A. M., N. Takemoto, E. J. Wherry, S. A. Longworth, J. T. Northrup, V. R. Palanivel, A. C. Mullen, C. R. Gasink, S. M. Kaech, J. D. Miller, L. Gapin, K. Ryan, A. P. Russ, T. Lindsten, J. S. Orange, A. W. Goldrath, R. Ahmed, and S. L. Reiner. 2005. Effector and memory CD8+ T cell fate coupled by T-bet and eomesodermin. *Nat. Immunol.* 6: 1236-1244.

34. Pearce, E. L., A. C. Mullen, G. A. Martins, C. M. Krawczyk, A. S. Hutchins, V. P. Zediak, M. Banica, C. B. DiCioccio, D. A. Gross, C. A. Mao, H. Shen, N. Cereb, S. Y. Yang, T. Lindsten, J. Rossant, C. A. Hunter, and S. L. Reiner. 2003. Control of effector CD8+ T cell function by the transcription factor Eomesodermin. *Science* 302: 1041-1043.

35. Lin, W., D. Haribhai, L. M. Relland, N. Truong, M. R. Carlson, C. B. Williams, and T. A. Chatila. 2007. Regulatory T cell development in the absence of functional Foxp3. *Nat. Immunol.* 8: 359-368.

36. Jenner, R. G., M. J. Townsend, I. Jackson, K. Sun, R. D. Bouwman, R. A. Young, L. H. Glimcher, and G. M. Lord. 2009. The transcription factors T-bet and GATA-3 control alternative pathways of T-cell differentiation through a shared set of target genes. *Proc. Natl. Acad. Sci. U. S. A.* 106: 17876-17881.

37. O'Shea, J. J. and W. E. Paul. 2010. Mechanisms underlying lineage commitment and plasticity of helper CD4+ T cells. *Science* 327: 1098-1102.

38. Zhou, L., M. M. Chong, and D. R. Littman. 2009. Plasticity of CD4+ T cell lineage differentiation. *Immunity* 30: 646-655.

39. Fazilleau, N., L. Mark, L. J. McHeyzer-Williams, and M. G. McHeyzer-Williams. 2009. Follicular helper T cells: lineage and location. *Immunity* 30: 324-335.

40. King, C., S. G. Tangye, and C. R. Mackay. 2008. T follicular helper (TFH) cells in normal and dysregulated immune responses. *Annu. Rev. Immunol.* 26: 741-766.

41. Miyara, M., Y. Yoshioka, A. Kitoh, T. Shima, K. Wing, A. Niwa, C. Parizot, C. Taflin, T. Heike, D. Valeyre, A. Mathian, T. Nakahata, T. Yamaguchi, T. Nomura, M. Ono, Z. Amoura, G. Gorochov, and S. Sakaguchi. 2009. Functional delineation and differentiation dynamics of human CD4+ T cells expressing the FoxP3 transcription factor. *Immunity* 30: 899-911.

42. Koch, M. A., G. Tucker-Heard, N. R. Perdue, J. R. Killebrew, K. B. Urdahl, and D. J. Campbell. 2009. The transcription factor T-bet controls regulatory T cell homeostasis and function during type 1 inflammation. *Nat. Immunol.* 10: 595-602.

43. Zhou, X., S. L. Bailey-Bucktrout, L. T. Jeker, C. Penaranda, M. Martinez-Llordella, M. Ashby, M. Nakayama, W. Rosenthal, and J. A. Bluestone. 2009. Instability of the transcription factor Foxp3 leads to the generation of pathogenic memory T cells in vivo. *Nat. Immunol.* 10: 1000-1007.

44. Bending, D., H. De La Pena, M. Veldhoen, J. M. Phillips, C. Uyttenhove, B. Stockinger, and A. Cooke. 2009. Highly purified Th17 cells from BDC2.5NOD mice convert into Th1-like cells in NOD/SCID recipient mice. *J. Clin. Invest.*

45. Djuretic, I. M., D. Levanon, V. Negreanu, Y. Groner, A. Rao, and K. M. Ansel. 2007. Transcription factors T-bet and Runx3 cooperate to activate Ifng and silence Il4 in T helper type 1 cells. *Nat. Immunol.* 8: 145-153.

46. Mullen, A. C., A. S. Hutchins, F. A. High, H. W. Lee, K. J. Sykes, L. A. Chodosh, and S. L. Reiner. 2002. Hlx is induced by and genetically interacts with T-bet to promote heritable T(H)1 gene induction. *Nat. Immunol.* 3: 652-658.

47. Hultgren, B., X. Huang, N. Dybdal, and T. A. Stewart. 1996. Genetic absence of gamma-interferon delays but does not prevent diabetes in NOD mice. *Diabetes* 45: 812-817.

48. Trembleau, S., G. Penna, S. Gregori, H. D. Chapman, D. V. Serreze, J. Magram, and L. Adorini. 1999. Pancreas-infiltrating Th1 cells and diabetes develop in IL-12-deficient nonobese diabetic mice. *J. Immunol.* 163: 2960-2968.

49. Bour-Jordan, H., B. L. Salomon, H. L. Thompson, G. L. Szot, M. R. Bernhard, and J. A. Bluestone. 2004. Costimulation controls diabetes by altering the balance of pathogenic and regulatory T cells. *J. Clin. Invest.* 114: 979-987.

50. Janes, K. A., J. G. Albeck, S. Gaudet, P. K. Sorger, D. A. Lauffenburger, and M. B. Yaffe. 2005. A systems model of signaling identifies a molecular basis set for cytokine-induced apoptosis. *Science* 310: 1646-1653.

51. Wei, G., L. Wei, J. Zhu, C. Zang, J. Hu-Li, Z. Yao, K. Cui, Y. Kanno, T. Y. Roh, W. T. Watford, D. E. Schones, W. Peng, H. W. Sun, W. E. Paul, J. J. O'Shea, and K. Zhao. 2009. Global mapping of H3K4me3 and H3K27me3 reveals specificity and plasticity in lineage fate determination of differentiating CD4+ T cells. *Immunity* 30: 155-167.

Figure

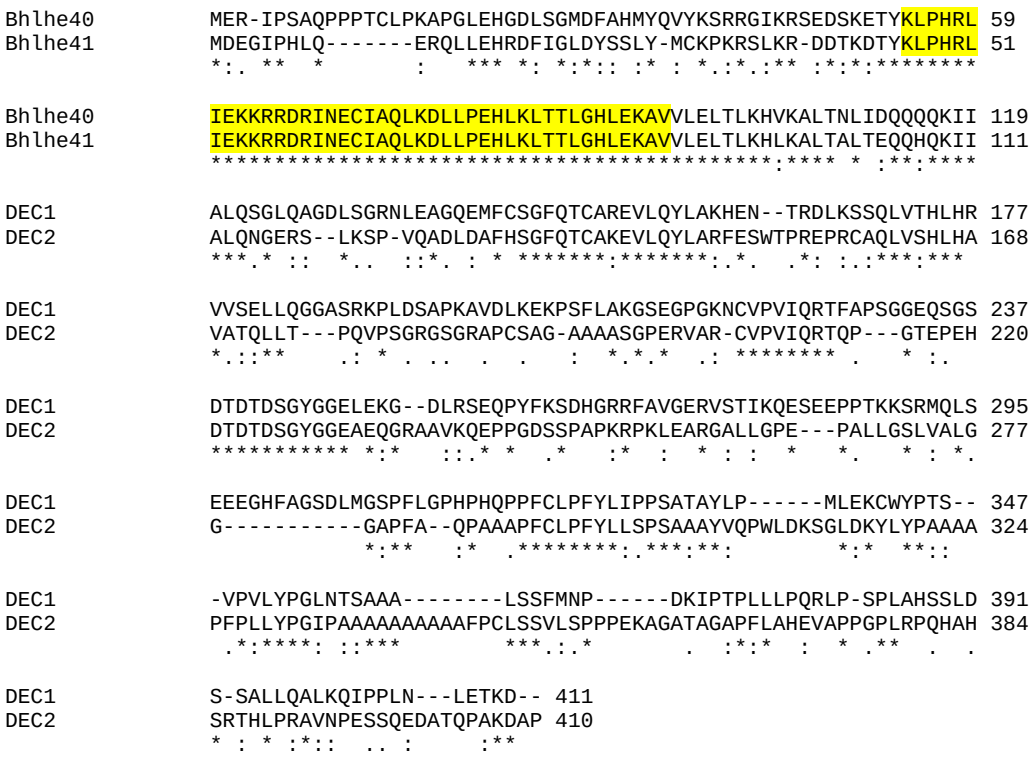

Figure 4.1: Alignment (using ClustalW) of the protein sequence of *M. musculus* Bhlhe40 and Bhlhe41. The basic helix-loop-helix binding domain is highlighted.

Publishing Agreement

It is the policy of the University to encourage the distribution of all theses, dissertations, and manuscripts. Copies of all UCSF theses, dissertations, and manuscripts will be routed to the library via the Graduate Division. The library will make all theses, dissertations, and manuscripts accessible to the public and will preserve these to the best of their abilities, in perpetuity.

I hereby grant permission to the Graduate Division of the University of California, San Francisco to release copies of my thesis, dissertation, or manuscript to the Campus Library to provide access and preservation, in whole or in part, in perpetuity.

Jonathan Haynes Esenstein 6/1/2010

Author Signature Date